Technology Collaboration Programme on Heat Pumping Technologies (HPT TCP)

Annex 41

Cold Climate Heat Pumps

Improving low ambient temperature performance of air-source heat pumps

Executive Summary

Operating Agent: The United States

2017

HPT-AN41-SUM

PART 1: EXECUTIVE SUMMARY

1 INTRODUCTION TO ANNEX 41

In 2012 the International Energy Agency (IEA) Heat Pump Programme (HPP; now HPT, Heat Pumping Technologies Programme) established Annex 41 to investigate technology solutions to improve performance of heat pumps for cold climates. Four IEA HPP member countries are participating in the Annex – Austria, Canada, Japan, and the United States (U.S.). The principal focus of Annex 41 is on electrically driven air-source heat pumps (ASHP) since that system type has the lowest installation cost of all heat pump alternatives. They also have the most significant performance challenges given their inherent efficiency and capacity issues at cold outdoor temperatures. Availability of ASHPs with improved low ambient performance would help bring about a much stronger heat pump market presence in cold areas, which today rely predominantly on fossil fuel furnace heating systems.

During the mid-1970s, following the first oil embargo, interest in use of heat pumps to provide space heating began to increase in much of the developed world (OECD countries). Many northern U.S. electric power companies began experiencing increasing peak kilowatt (kW) demands during the heating season as shortages of natural gas and oil led to increased usage of direct electric heating. In response they began investigating the use of ASHPs as a means of mitigating the increased peak demands. ASHPs are almost universally applicable to buildings in all parts of the world and, given that they were the primary type available, were of main interest as an alternative electrical heating system at that time. However, as noted above, they suffer both heating capacity (output) and efficiency (coefficient of performance or COP) degradation as the outdoor ambient temperature drops while at the same time the building heat demand is increasing. As such, ASHPs require a supplemental heating source – usually direct electric resistance heating elements – to bridge the gap between the building heat demand and the ASHP heating output. This feature causes lower seasonal performance and limits peak electric demand reduction potential leading to limited acceptance of ASHPs in areas that experience large numbers of hours at cold temperatures (loosely defined as ≤ -7°C for purposes of Annex 41). In addition, typical heat pump compressors fail to work at extremely low ambient temperatures due to the significantly high pressure ratios and discharge temperatures. A primary criterion for ASHPs to achieve good seasonal performance in cold areas is, therefore, achieving high heating output (capacity) at low ambient temperatures so as to minimize reliance on supplemental heat sources and maximize the overall system heating seasonal performance factor (HSPF in Btu/Wh or the dimensionless equivalent SCOP).

For the reasons noted above, ASHPs have been the primary heat pump type of interest for Annex 41. However, ground source and solar-assisted heat pumps (GSHP and SAHP) have also been addressed by some of the participants. A primary technical objective of the Annex is to define pathways to enable ASHPs to achieve an "in field" $SPF_h \geq 2.63$ W/W (HSPF ≥9.0 Btu/Wh), the minimum level necessary in order to gain recognition as a renewable technology in the European Union.

As stated in the 27 February 2013 legal text for the Annex the work was divided into four main tasks:

- <u>Task 1: Critical literature survey</u> – Participants undertook a literature review and review of results from prior related research to identify candidate ASHP system design possibilities for further evaluation and study.
- <u>Task 2: System design and application studies - modeling and/or laboratory-controlled measurements</u> - The focus was on detailed analyses of promising component/system concepts including outdoor heat exchanger frosting/defrosting issues considering the system performance and cost implications as well as design

and control issues. Laboratory prototype and field prototype testing may be included in this task as well.

- Task 3: Simulations of energy savings impacts of prototype advanced ASHP design - This task involved seasonal/annual performance simulations based on the Task 2 studies to estimate energy and emissions savings potential.
- Task 4: Report and information dissemination - Each participant has provided a final country report addressing their respective results from the tasks above. These have been assembled into this final Annex report by the Operating Agent. A number of possible further areas for study are included.

Annex members have focused on two primary areas to address the cold climate performance problems noted above. First, advanced Cold Climate Heat Pumps (CCHPs) with low-temperature capacity-enhancement approaches have been developed. Secondly, detailed analytical and experimental investigations on outdoor heat exchanger (OHX) frosting have been conducted, primarily by the Japanese and Austrian teams.

1.1 Objectives

This project is primarily focused on electrically-driven ASHPs with air or hydronic heating systems (e.g., air-to-air or air-to-water heat pumps) since these products have the greatest challenge in providing sufficient heat output and maintaining high efficiency levels at lower outdoor temperatures. Electric ASHPs generally have the lowest installation cost of all heat pump alternatives, but also the greatest performance challenges at cold outdoor temperatures. One of these is loss of heating capacity. Traditional ASHPs lose 80% of their heating capacity at outdoor temperatures of -25°C compared to the rated performance at 8.3°C. This means that traditional ASHPs must use low-efficiency backup heat at lower temperatures, as noted in Figure ES-1. The other major issue is the loss of capacity due to frosting and defrosting of the outdoor heat exchanger (OHX) at moderate outdoor temperatures between about -5°C to 5°C (noted in Figure ES-1).

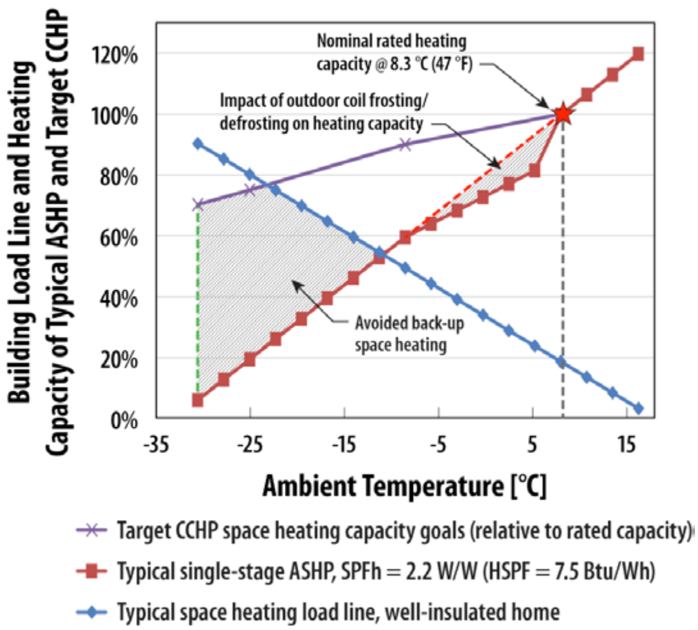

Figure ES-1: Space heating capacity for target CCHP (per Table ES-1 below) vs. typical single-stage ASHP

Technical performance goals for CCHPs as established by the U.S. Department of Energy's Building Technology Office (DOE/BTO) are listed in Table ES-1.

Table ES-1: U.S. CCHP performance targets

Outdoor Temperature	Heating Capacity
8.3°C (47°F)	9-21 kW (2.5-6 tons), nominal rating
-25°C (-13°F)	≥75% of nominal rating

A major technical objective as stated in the Annex legal text is to identify solutions that can lead to improved ASHPs for cold climate application with a heating SPF ≥ 2.63 W/W, the minimum level necessary in order to gain recognition as a renewable technology in the EU.

These objectives have parallel interest under the IEA Framework of Implementing Agreements (now Technology Collaboration Partnerships, TCP) as the intent is to identify, quantify, and deliver information to key industry stakeholders and policy makers and to provide pertinent resources to building owners and operators. The objectives will be achieved by independent studies and investigations performed by the country-specific participants. The main output of this Annex is information sharing on viable means to improve ASHP heating performance under cold ambient temperature conditions so that better cross-country understanding is achieved to reduce energy consumption (and the related CO_2-emissions) while satisfying the needs of building owners and operators.

1.2 Target Audience and Benefits

The sectors targeted for this Annex include:

- HVAC practitioners responsible for designing, selecting, and sizing heat pump systems in varied applications with a focus on cold ambient locations.
- Building owner/operators in cold regions interested in achieving improved comfort conditioning and efficiency performance from their HVACR equipment.
- Entities charged with minimizing energy utilization (i.e., utilities, utility commissions, energy agencies, legislative bodies, etc.) in varied heat pump applications and geographic conditions.

1.3 Annex Activities and Time Schedule

Table ES-2 breaks down Annex 41 tasks and time schedule.

Table ES-2: Annex 41 tasks and time schedule (actual)

Start Date	End Date	Annex 41 Activities
July 2012	March 2013	Task 1 – Critical literature survey
Dec 2012	June 2015	Task 2 – System design and application studies - modeling and/or laboratory-controlled measurements
June 2014	March 2017	Task 3 – Simulations of energy savings impacts of prototype advanced ASHP design
Jan 2013	July 2017	Task 4 – Report and information dissemination

1.4 Summary of Principal Outcomes

Table ES-3 summarizes the principal outcomes resulting from the activities of each Annex participant.

Table ES-3: Principal outcomes of performance improvement techniques investigated by Annex participants

Annex Participants	**CCHP Investigated Techniques**	**Resulting Performance Improvements**	**Reference**
Austria (AIT)	Coil frost measurements and analyses	• Wind tunnel tests of outdoor heat exchangers (OHX) show multiport extrusion (MPE) compact heat exchangers experience less air flow reduction due to frost growth than conventional tube-and-fin (CTF) heat exchangers at both 10°C and -25°C air temperature (80% RH in both cases); therefore, they can maintain better air flow.	Reichl, et al., 2015; Strehlow, et al., 2015; Popovac, et al., 2015a; Popovac, et al., 2015b
Austria (Technical University, Graz)	Evaluation of compressor liquid injection (LI) for cold climate performance improvement	• Lab tests show LI capability to extend compressor performance envelope for air-water heat pumps down to -20°C or lower with high water supply temperatures • System analyses for several cold climate locations show seasonal COP improvements of up to 12%	Hengel et al., 2013; Zoier,2014; Moisi, et al., 2015
Canada (CanmetENERGY)	Novel SAHP (solar-assisted HP) using ice-based thermal storage	• Lab tests/simulations estimate >60% space and water heating energy savings potential • Potential cost-effective alternative to GSHPs in Canadian climates especially for retrofit applications	Tamasauskas, et al., 2012
	Zeotropic refrigerant mixtures	• Evaluations of potential for zeotropic mixture of R32 and CO2 to improve system efficiency and low temperature capacity • Results show possibility of ~30% seasonal COP improvement with variable mixture composition control components included in heat pump system • Plans to build & test lab prototype	Hakkaki-Fard, et al., 2014; Hakkaki-Fard, et al., 2016
Canada (Hydro Quebec LTE)	Revisions to seasonal efficiency rating standard to better represent heat pump performance in cold climates	• Field testing of ASHP systems pointed out inadequacies in seasonal efficiency rating metrics per Canadian Heat Pump rating standard CAN/CSA-C656-05 for cold climate applications • Office of Energy Efficiency issued bulletin requiring changes in ASHP heating performance ratings and reporting; specifically required adding capacity and COP ratings for -17.8 °C outdoor temperatures by 2014.	NRCan 2010, Office of Energy Efficiency Bulletin 7177, Reporting Cold Climate Performance,
Japan	Coil surface frosting R&D (Waseda University)	• Innovative frost growth measurement & visualization technique (resolution to 0.02 mm) • Frost growth model developed; comparison with measurements for	Yasui, et al 2017 (Conference paper O.1.6.2); Yamashita, 2009; Tao, et al., 1994; Le Gall, et al., 1997

Annex Participants	CCHP Investigated Techniques	Resulting Performance Improvements	Reference
		different surface geometries • Applied frost model to heat pump system model; coil frost growth measured vs. simulated	
	Novel frost-free air source heat pump water heater (ASHPWH) system (Central Research Institute of the Electric Power Industry, CRIEPI)	• System retards frosting by dehumidifying air using a desiccant-coated heat exchanger • Potential for 20-30% boost in COP at a temperature of -7°C and relative humidity of 60-80%.	Zhang, et al., 2017 (Conference paper O.1.6.3)
United States	Two (parallel, equal-sized) compressor field test CCHP prototype (ORNL, Emerson)	• Achieved measured $SCOP_h$ ~3.0 over two winters (2015 and 2016) • 40% energy savings in coldest month; possible to eliminate backup electric heat • Heating COP at -25°C was >2.0; ~3.8 at 8.3°C (including cycling losses)	Shen, et al., 2017 (Conference paper P.1.5.6); Shen et al., 2014
	Novel oil-flooded HP cycle development and evaluation (Purdue University Herrick Labs)	• Approaches isothermal vapor compression process • High oil circulation rates remove heat of compression & significantly reduce discharge temperature, which expanded compressor operation envelope to much lower ambient temperatures • Improvements in heating capacity range up to 19% at the lowest ambient temperature tested (-17.8°C)	Bell, et al., 2011; Yang, et al., 2014; Ramaraj, et al., 2016
Complementary market promotion activities*	U.S. Northeast Energy Efficiency Partnership	• Established voluntary CCHP specification; latest version (2017) posted on NEEP web site (see next column) • For variable speed (VS) ASHPs only; requires rated SCOPh ≥2.93 per ANSI/AHRI Standard 210/240 • Web site contains list of nearly 300 ASHPs that meet the requirements; 80% are ductless minisplit or multisplit (VRF) types	Northeast Energy Efficiency Partnerships, 2017
[*These efforts were conducted independently of the Annex but took place during the Annex working	U.S. Electric Power Research Institute (EPRI), Next Generation (NextGen) Heat	• ASHPs only but VS compressor not required; other capacity control approaches acceptable • Two levels of NextGen specification requirements • Tier 1 requires same rated SCOPh as NEEP CCHP spec above; rated	Domitrovic, 2017

Annex Participants	**CCHP Investigated Techniques**	**Resulting Performance Improvements**	**Reference**
period and will continue for foreseeable future]	Pump specifications	heating capacity at -8.3°C to be ≥80% of rated capacity at 8.3°C; requires control scheme to limit backup heat use; must have demand response capability • Tier 2 requires rated SCOPh ≥3.81; rated heating capacity at -15°C to be ≥80% of rated capacity at 8.3°C; requires control scheme to limit backup heat use; must have demand response capability; only ~7% of ASHPs listed on NEEP site currently meet Tier 2 requirements	

2 COUNTRY SPECIFIC SIGNIFICANT RESULTS AND FINDINGS

2.1 Austria

Two primary research teams comprise the Austrian Annex 41 team. One is the team at the Center for Energy, Austrian Institute of Technology (AIT) in Vienna, led by Dr. Thomas Fleckl and Dr. Christoph Reichl. The other is the Institute of Thermal Engineering (IWT, Institut für Wärmetechnik) of the Graz University of Technology (TU Graz), led by Dr. René Rieberer.

2.1.1 TU Graz contributions

Simulation work has been carried out at IWT in order to investigate the potential of nine different heat pump cycles for cold climate applications, shown in Table ES-4. Simplified simulation models of promising heat pump layouts have been carried out using the Engineering Equation solver (EES) program in order to increase the range of application and efficiency. The investigated refrigerant was R410A.

Table ES-4: Investigated cycle layouts and parameters (according to Zoier, 2014)

Model No.	Description	Stages	Additional parameters
01	Conventional cycle	1	-
02	Cycle with internal heat exchanger (IHX)	1	Efficiency of IHX
03	Cycle with flooded evaporator, low pressure (LP) accumulator (separator)	1	Pump efficiency, Pressure drop in LP cycle
04	Two stage cycle with intercooler	2	Temperature difference to saturation curve, intermediate pressure level (IP)
05	Liquid injection cycle	1	Intermediate pressure level, injection mass flow
06	Vapor injection with internal heat exchanger (IHX or Economizer_IHX)	2	Efficiency of IHX , intermediate pressure level
07	Vapor injection with receiver (Economizer_receiver)	2	intermediate pressure level
08	Cascade system	2	Temperature difference between low and high temperature (HT) cycle, refrigerant
09	Ejector cycle	1	Ejector efficiency

The cascade cycle has shown COP improvements up to 5% compared to the conventional cycle. Vapor injection (VI) with flash tank or with an internal heat exchanger (IHX) shows a COP increase in the range of 4% and 10%, respectively, at -30°C evaporation temperature. The work of Hengel et al. (2013) also showed slight COP improvements for the economizer with internal heat exchanger, especially at higher heating supply temperatures. Intercoolers show a rather high decrease of COP and heating capacity if the heat removed from the intercooler is not used. The IHX cycle resulted in similar values as the conventional cycle and showed no improvement in any category. The liquid injection (LI) cycle caused minor COP losses in a range of 2% but identical heating capacity compared to the conventional cycle. The resulting compressor outlet temperatures could have been decreased within all models except the IHX cycle. The most promising layouts in this regard are cascade, intercooling, and LI, with a drop in compressor outlet temperatures of 19 K, 21 K and 32 K respectively compared to the conventional cycle at an evaporation temperature of -30 C.

An investigation of the LI cycle by Lammert (2013) noted the possibility to enable a significantly larger compressor operation envelope by lowering the compressor discharge temperature, which is of special interest in case of high condensation temperatures (see Figure ES-2). Overall the LI concept does not offer as great an improvement to ASHP efficiency and capacity as does for instance the vapor injection (VI) approach, but it does offer a rather simpler means to allow ASHPs to operate at very low ambient temperatures. This may result in ~10% energy savings compared to a standard heat pump combined with a furnace heating backup (Lammert, 2013).

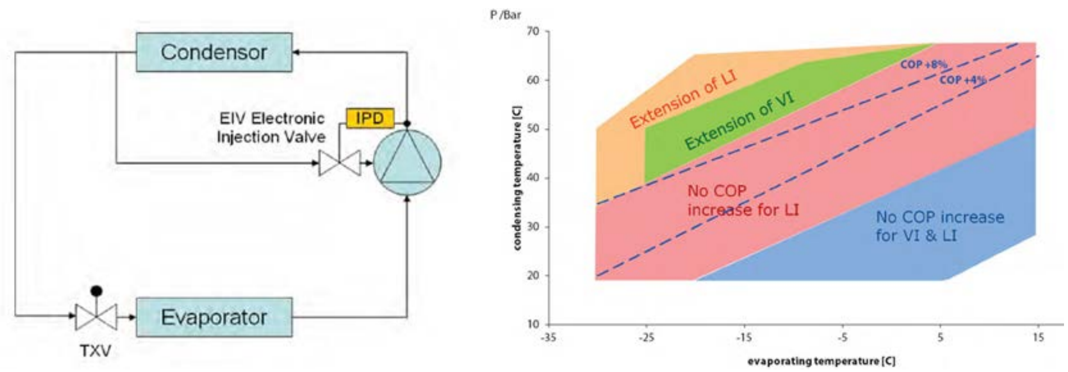

Figure ES-2: Liquid injection: basic layout (left); compressor envelope (right) (Lammert, 2013)

Based on the simplified calculations, a more detailed model of the LI cycle was set up. For the calculation of the heat transfer, the evaporator and condenser are divided into different sections considering phase transformation (gaseous, two phase and liquid). Estimated supplier provided U-values have been applied for each individual section. Moreover, area fractions of the heat exchangers for each section depending on the pressure level and temperatures are calculated to estimate the two-phase flow along the heat exchanger. Initial temperatures derived from ambient temperature and water outlet temperature are applied to start the pressure iteration process. The refrigerant mass flow as well as isentropic efficiencies for the high and low pressure stage can be calculated according to polynomial functions given by manufacturer data in dependence of p_{evap} and p_{cond}. The air volume flow is also given by manufacturer data and remained constant. The state of ambient air has been defined by temperature, pressure and relative humidity. The injection is controlled by means to a temperature threshold. If the discharge temperature of the high stage compressor is below this threshold, injection is inactive. The injection mass flow can then be calculated iteratively by comparison of the current discharge temperature (T_{cond_in}) with the set maximum compressor outlet temperature (T_{VI}).

The LI cycle was been chosen for more detailed study for two primary reasons. First, it has a less complex layout compared to the cascade and economizer systems. Secondly, it has the ability to increase the range of heat pump application for cold climates in terms of compressor outlet temperature. Furthermore, a LI prototype air-to-water heat pump (AWHP) was available to carry out experimental analysis. The detailed model considers heat transfers on the heat sink and heat source heat exchanger and calculates the resulting evaporation/condensation pressure level iteratively. Furthermore polynomial functions provided by manufacturer data are used to describe the volumetric efficiency of the compressor and the isentropic efficiencies based on evaporation and condensation temperature.

Lab test results with the LI prototype (Zoier, 2014) are shown in Figure ES-3. The effect of the refrigerant injection on compressor discharge temperature is clear especially for the highest water outlet temperatures (W55 and W60). The injection allows an extension of compressor operation for low ambient temperatures, especially at high water temperatures and thus pressure ratios as suggested by the analyses. The discharge temperatures under the lower water outlet temperature conditions (W35 and W45) were below the defined threshold (125°C) for LI activation at all times hence the refrigerant injection was not active. However, the discharge temperature at -19°C and W45 was 126°C without injection activation which might be caused by a measurement error.

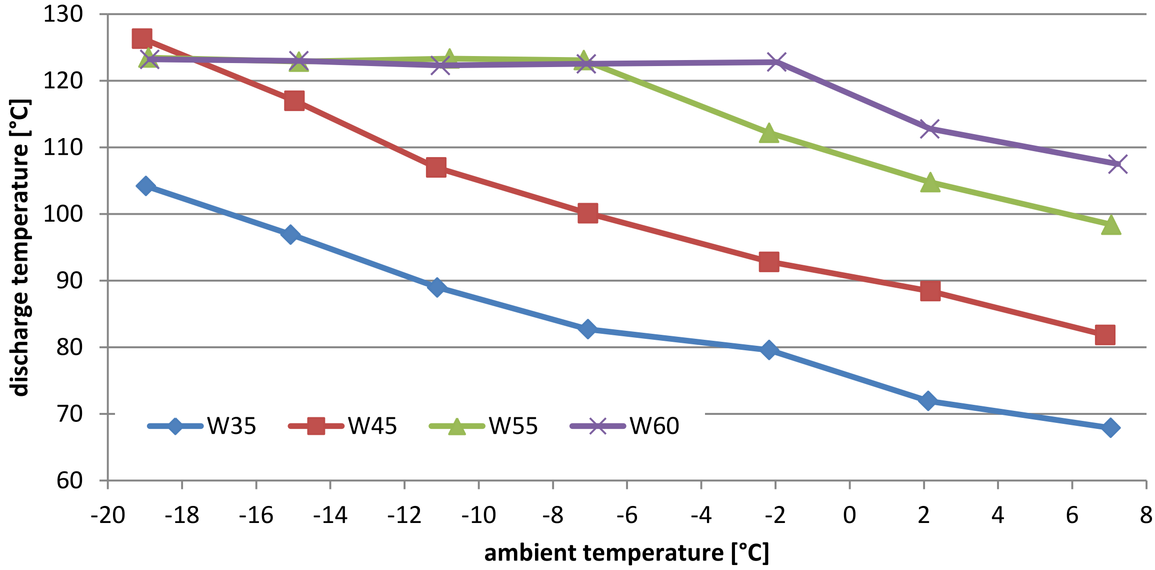

Figure ES-3: Discharge temperature in dependence of water outlet and ambient temperature according to Zoier (2014)

An assessment of an LI cycle AWHP system was conducted to calculate energy savings compared to a conventional AWHP without LI in five cities (Anchorage, Graz, Helsinki, Minneapolis, and Moscow). It must be noted that while the results are overestimated quantitatively compared to the experimental data (Moisi et al., 2015), they do illustrate a qualitative trend. With a water supply temperature of 35°C, no injection is needed at all and no difference was seen between the SPF results for the conventional and LI AWHP systems. A difference between the conventional and the LI systems is observed at a water supply temperature of 45°C (Figure ES-4). With increasing operation time of the LI System at lower ambient temperatures (approx. below -20°C), the SPF improvement compared to the conventional system increases since no backup heater is necessary. In the case of Minneapolis for example, an SPF improvement of 12% can be achieved compared to the conventional system. On the other hand, Graz shows no effect at all since the minimum ambient temperature is too high for the activation of liquid injection (approx. -12°C). However, the threshold ambient temperature for the injection activation is dependent on the control strategy. Another fact is clear, that with an increasing heat supply temperature this threshold rises to higher ambient temperatures. Therefore, a liquid injection system can be interesting for more moderate climates and high temperature heating systems in the course of refurbishments in order to realize a monovalent heating system as well as for hot water production.

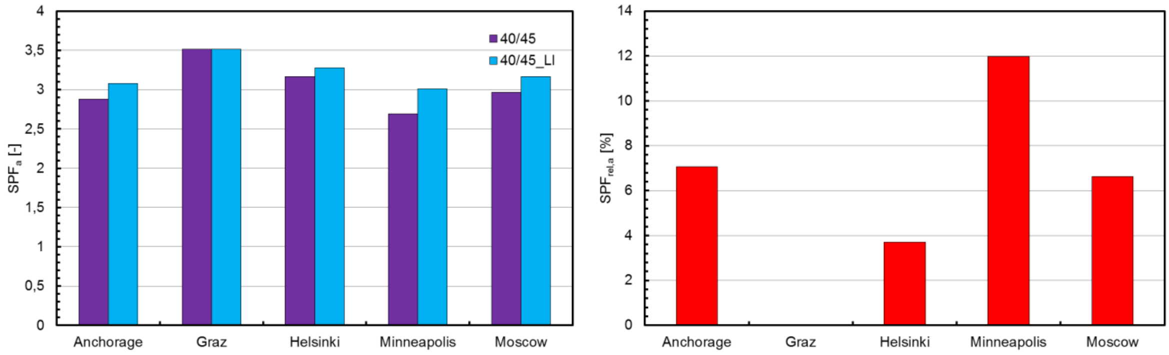

Figure ES-4: Comparison of SPF (left) and relative SPF improvement (right) for LI and conventional AWHPs with a 45°C water supply

A LI system can increase the range of application to lower ambient temperatures. Compared to a conventional air source heat pump system with a direct electrical backup heater, annual efficiencies can be improved depending on the time the heat pump operates at lower ambient temperatures.

2.1.2 AIT contributions

The AIT team technical contributions to Annex 41 focus on improving AWHP evaporator performance. This is a part of the EU Green Heat Pump Project (EU-FP7 research project) coordinated by AIT with contributions from several European industrial partners as well as research institutes (Zottl, 2016). Figure ES-5 illustrates the overall EU-FP7 project approach.

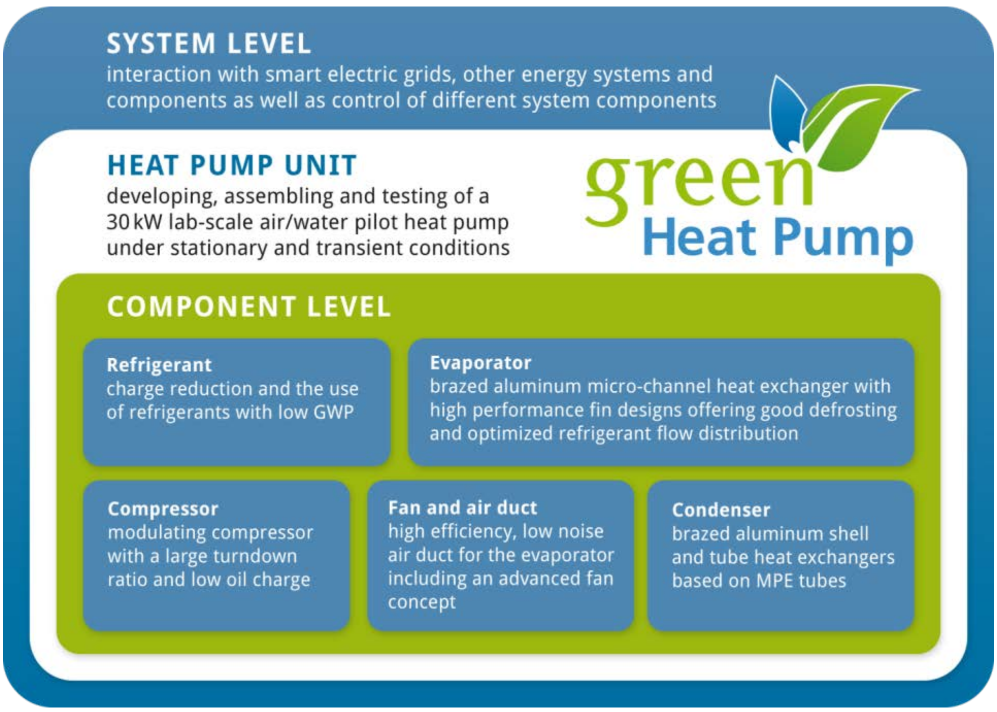

Figure ES-5: EU-FP7 Green Heat Pump project objectives (Zottl, 2016)

AIT's research activities were focused on the investigation of evaporator frosting in cold climates, in search of an evaporator design with good frosting/defrosting performance and optimized refrigerant distribution. A small-scale wind tunnel test apparatus was constructed at AIT for experimental evaluation of the frosting performance of candidate fin designs for the system multiport extrusion (MPE) compact heat exchanger evaporator design. Figures

ES-6 and ES-7 show a photograph and schematic of the wind tunnel. Seven different fin designs were mounted on an MPE tube and tested in the wind tunnel. Figure ES-8 and Table ES-5 illustrate a sample MPE compact heat exchanger with the tested fin characteristics and dimensions. Results for icing time (t_{ICE}; the longer, the better) and average heat transfer duty (the greater, the better) are shown in Table ES-6. Both wavy fin designs showed reasonable balance between long icing times and high mean heat transfer, and are recommended for the system evaporator designs.

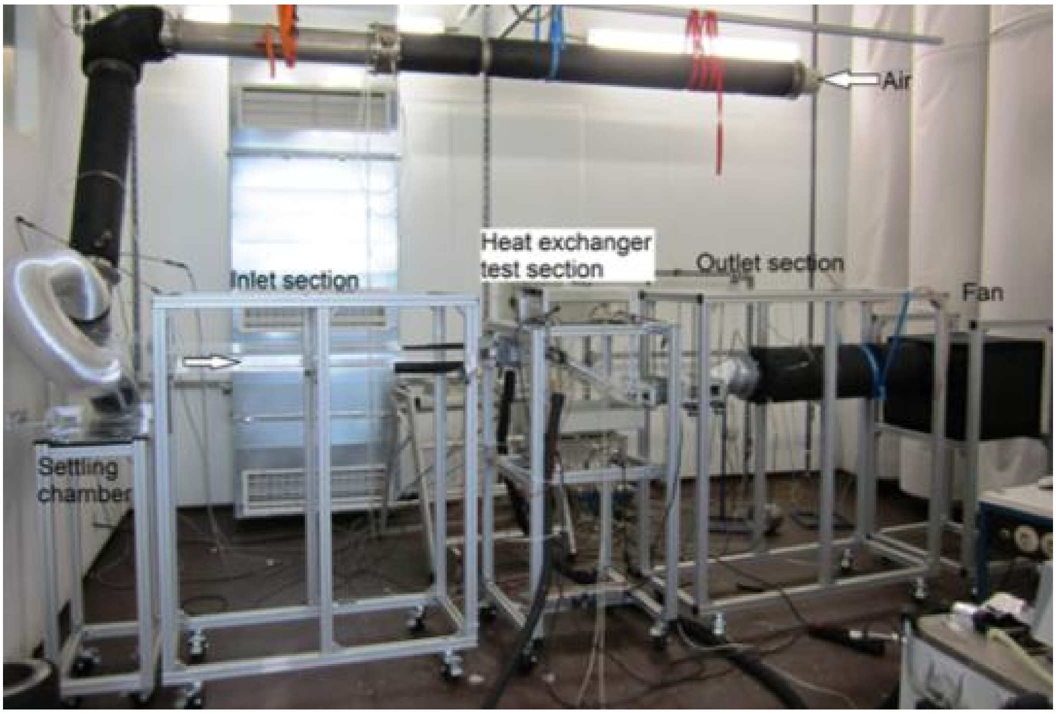

Figure ES-6: Small-scale wind tunnel at AIT (Zottl, 2016)

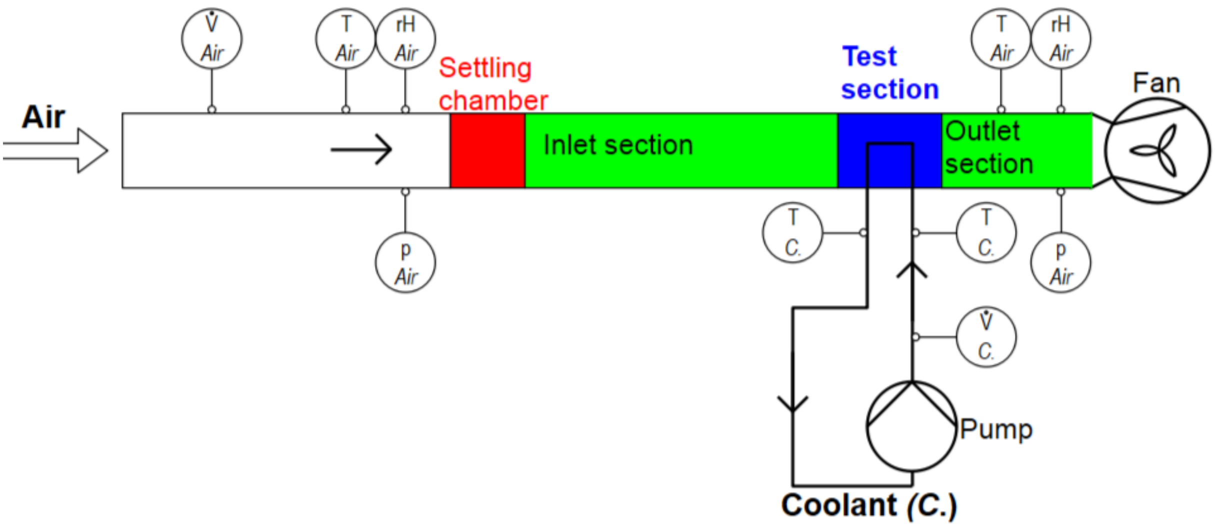

Figure ES-7: Wind tunnel diagram showing instrumentation scheme (Zottl, 2016)

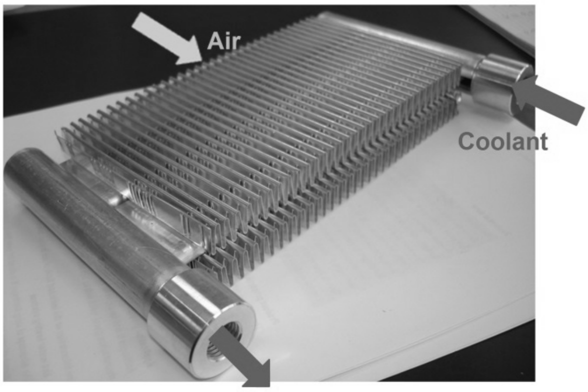

Figure ES-8: Typical fin sample with wavy fins mounted on a MPE tube

Fin / Name of the sample	Height	Pitch
Plain fin #1	10,4 mm	5,0 mm
Plain fin #2	10,4 mm	10,0 mm
Wavy fin #1	10,4 mm	5,0 mm
Wavy fin #2	10,4 mm	8,0 mm
Lanced fin #1	10,0 mm	4,8 mm
Louvered fin #1	10,4 mm	5,3 mm
Plain/louvered fin #1	10,4 mm	--

Table ES-5: Summary of fin samples tested

Fin / Name of the sample	Mean values t_{ICE}	Mean values $\dot{Q}_{mean}$
Plain fin #1	3059 s	156 W
Plain fin #2	4688 s	104 W
Wavy fin #1	2380 s	166 W
Wavy fin #2	3767 s	135 W
Lanced fin #1	1300 s	163 W
Louvered fin #1	1766 s	167 W
Plain/louvered fin #1	883 s	117 W

Table ES-6: Fin frosting performance test results (Zottl, 2016)

Wind tunnel tests determined that the MPE heat exchangers have better frosting characteristics than conventional tube-and-fin (CTF) heat exchangers. This can be seen in Figure ES-9, which depicts evaporator frost accumulation rate vs. time, and shows that the resulting reduction of air flow through the evaporator (relative to the maximum flow rate) is less for the MPE and the CTF case. The MPE evaporator has been included in research toward developing an innovative AWHP system prototype. Shown in Figure ES-10 is a comparison of measured frost distribution (left side) to simulated frost distribution (right side) resulting from the refrigerant temperature variation inside the evaporator. The view is looking from above onto the horizontally mounted heat-exchanger with refrigerant entering from the bottom of the figure. The blue bars indicate horizontal sums and vertical sums for each condensate weighing station. Horizontal bars to the left of the left-side graph show that frost builds up predominantly at the refrigerant entrance while the vertical bars indicate the extent of refrigerant fluid maldistribution. Simulation results on the right-hand side of Figure ES-10 are similar to the measured results on the left-hand side.

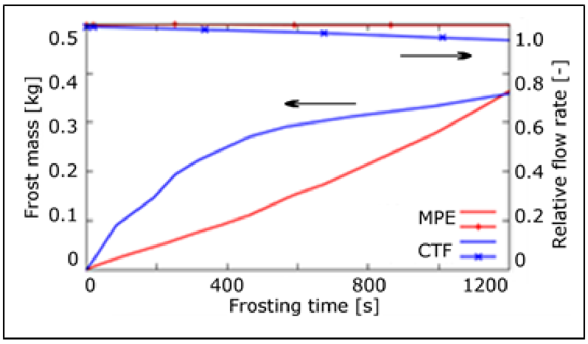

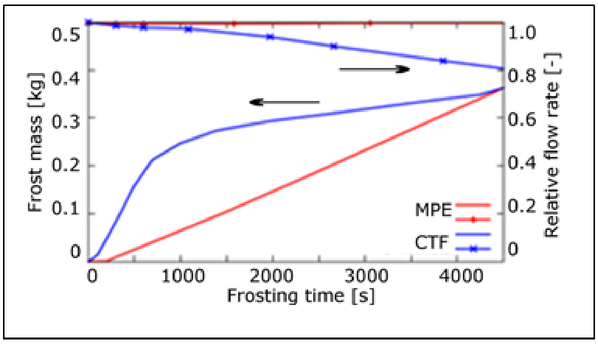

Figure ES-9: Frost mass growth and relative flow rate for advanced (MPE) and standard (CTF) heat exchanger configurations, at ambient temperatures 10°C (left) and -25°C (right)

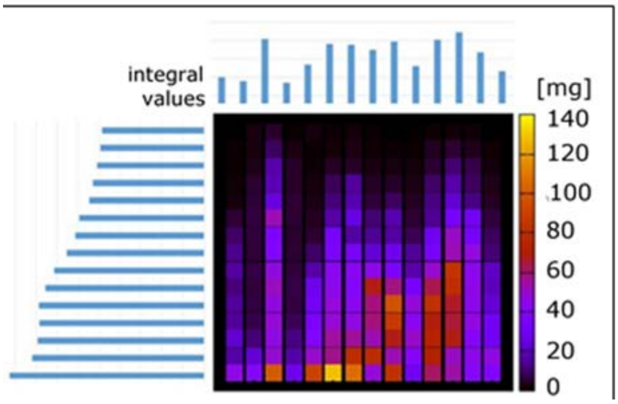

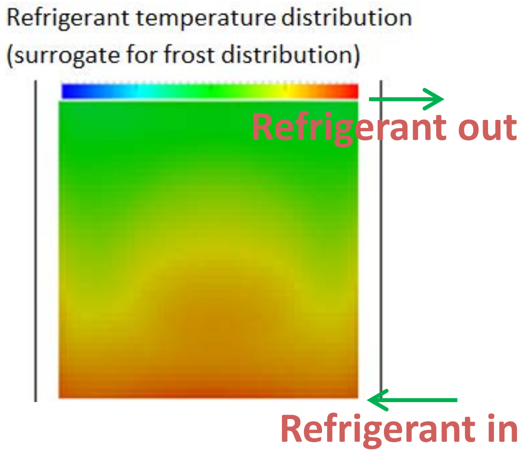

Figure ES-10: Measured (left) vs. simulated (right) frost distribution on MPE evaporator from AWHP system tests

2.2 Canada

Canada has two research institutes comprising its Annex 41 team. One is at CanmetÉnergie of National Resources Canada led by Dr. Daniel Giguère. The other is at the Laboratoire des Technologies de l'Energie (LTE) of Hydro-Québec led by Dr. Brice Le Lostec.

In Canada space heating is responsible for 64% and 50% of the energy use for residential and commercial buildings, respectively. Water heating is second with 17% and 8%, respectively. Heat pumps have potential to significantly reduce buildings energy use but current ASHP technology has poor performance in most Canadian locations, typically in cold or very cold climate regions. GSHPs can provide significant energy savings but are still too expensive to penetrate much of the Canadian market.

2.2.1 CanmetENERGIE Contributions

CanmetÉnergie's R&D activities related to CCHP technologies aim to improve the efficiency and cost effectiveness of several heat pump system types for the Canadian market. Their R&D for Annex 41 focused on four main areas (Giguère, 2014):

1. Advanced vapor compression (VC) cycles, with a focus on the ejector-compressor hybrid cycle
2. GSHP technology using carbon dioxide (CO_2) as the ground loop fluid and as the heat pump refrigerant

3. Solar-assisted heat pump (SAHP) system using an ice slurry fluid
4. Use of refrigerant mixtures with moderate to high temperature glides in ASHP systems

Ejector-Compressor Hybrid Cycle

While the hybrid ejector/compressor system is relatively simple in concept (Figure ES-11), the main development challenge lies in understanding well the two-phase-flow that takes place inside the ejector component. Current ejector research findings are not well described in the literature.

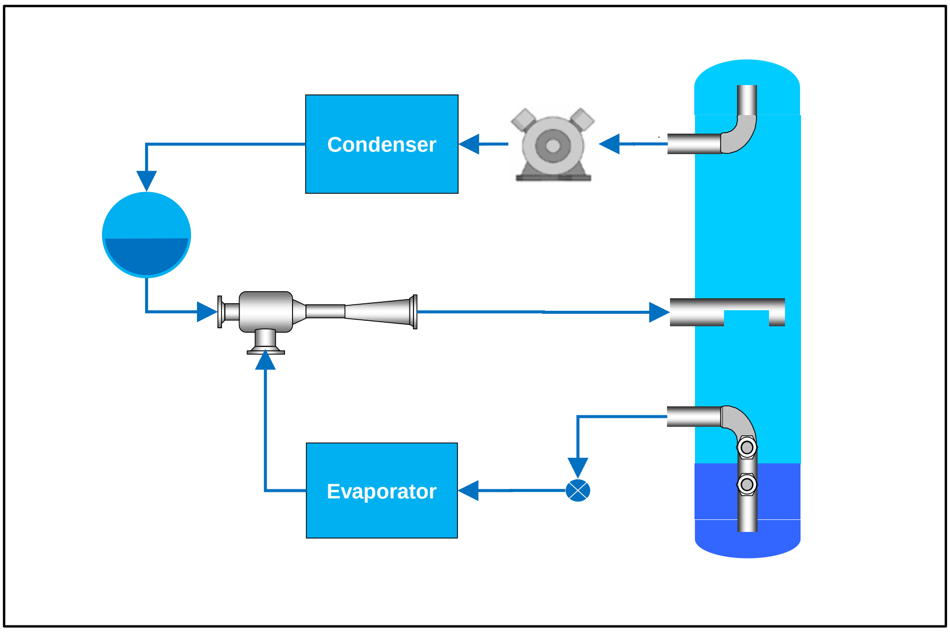

Figure ES-11: An example of a hybrid ejector/compression air-source HPs

To gain a better understanding of the two phase flow ejector and integration into a heat pump, a hybrid ejector/compressor test bench for heating applications was constructed and some tests performed under a previous research project. The test bench uses a variable speed compressor combined with an electronic expansion valve for maximum flexibility of operation. Its nominal heating capacity is 10 kW, which corresponds to the typical capacity of residential and light commercial applications. This test bench has been upgraded for this project with the refrigerant recently replaced from R410A to R134a due to partial fractionation occurring in the separator. Preliminary results have shown appropriate compression ratios; however, entrainment ratios would need to be improved. Our efforts are now directed towards the development of a better ejector for R134a (current ejector in test bench was designed for R410a) that will lead to higher entrainment ratios.

Coupled with the hybrid ejector/compressor test bench, a second test bench, dedicated solely to the study of the two phase ejector component was also constructed for this project. Capable of inducing a wide range of operating conditions, the two phase ejector test bench will generate in- depth knowledge and experimental results used to validate numerical models.

These experimental activities, coupled with the modeling work and validation of results, will significantly improve our knowledge on the design of two-phase-flow ejector components and heat pump systems.

Solar-Assisted Heat Pump System

SAHP systems, which rely on solar energy to supply or supplement heat pump operations, offer an attractive alternative to ASHPs and GSHPs more commonly found in the Canadian market. Solar based systems are often challenging to design and implement because they (i) require significant thermal storage capacity to bridge the temporal discrepancy between solar availability and thermal demand, and (ii) experience reduced collector efficiencies in the winter months when thermal demand in cold climates is highest. To address these issues, Canmet has worked extensively on the development of a new SAHP concept using ice-based latent storage.

Figure ES-12 is a schematic of the SAHP system (for both space heating and water heating) that was investigated by the team. The thermal storage tank in the schematic contains an ice slurry mixture that is circulated between the solar collectors and the evaporator of the heat pump when in SAHP operation mode.

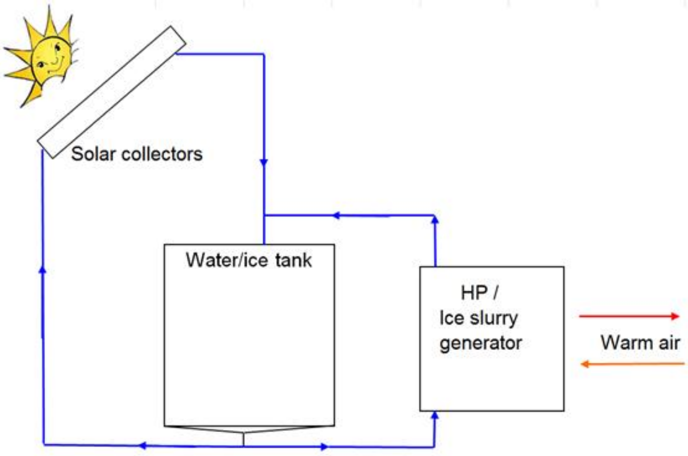

Figure ES-12: Solar-assisted heat pump system

Using validated energy models, it is estimated that such a system can reduce the energy use for space and domestic water heating in high performance homes between 61% and 66%, depending on the location of the building. Table ES-7 summarizes projected system sizing for typical existing homes in Eastern Canada. Provided that the ice generation/storage technology can be sourced at a reasonable cost, the proposed SAHP offers a cost-effective alternative to the current generation of GSHPs and is particularly interesting for retrofit applications where it may be difficult to add ground heat exchangers.

Table ES-7: Suggested SAHP design parameters for typical Canadian housing

Parameter	**Suggested Value/Range**
Solar Collector Area	30 m^2 to 40 m^2
Ice Storage Tank Volume	Approx. 5 m^3
Heat Pump/Ice Generator Capacity	10 kW (3 tons)

CO_2 in GSHPs

GSHPs are one of the most efficient commercially available space heating systems in Canada – typically yielding a high annual COP (~3) and reducing the space heating energy consumption by up to 65%. Typically high first costs remain a barrier to widespread market adoption and thus the main objective of the project is to find ways to reduce the initial investment cost or further increase the efficiency of the system to make it a more attractive solution. Furthermore, with the phase-out of HCFC refrigerants now in effect for new equipment and the next step phasing down HFC refrigerants, several projects are evaluating the feasibility of using CO_2 as the working fluid. CO_2 has a low global warming potential and the thermo-physical properties provide several advantages.

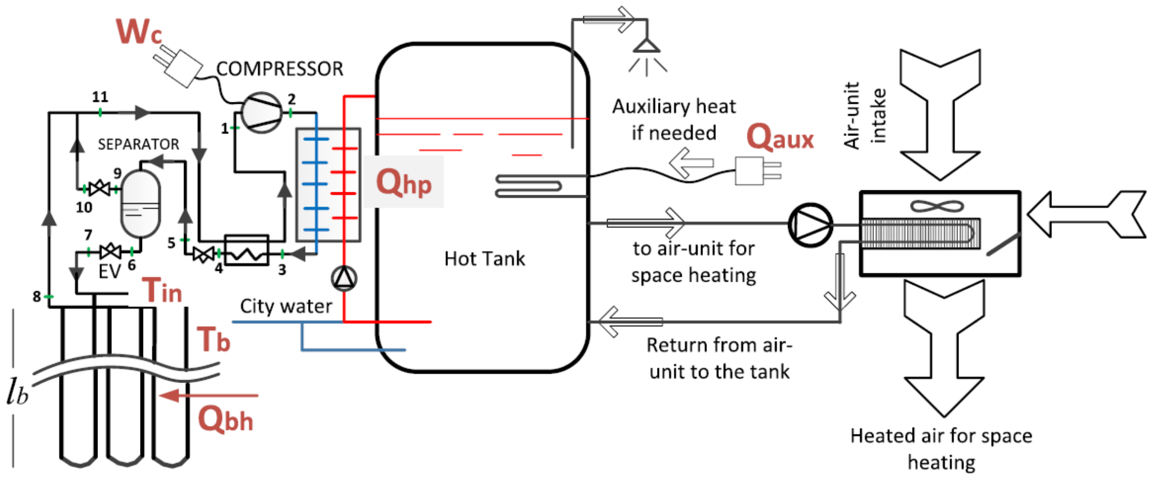

Figure ES-13: CO_2 GSHP-DX system

The objective of this work is to contribute to the advancement of underground heat extraction technologies using CO_2 as a phase change fluid carrier and to provide a cost effective and environmentally friendly alternative to GSHP systems commercially available today. One proposed configuration is as shown in Figure ES-13. The work consists of conducting experimental work on a new test bench at Canmet facility and developing simulation models to support the optimization of CO_2 ground loop configuration and operation.

CO_2 is much less sensitive to pressure drop than synthetic refrigerants, which enables the downsizing of the borehole U tube diameter. The underground heat exchanger performance is 13.6 m/kW, which compares favorably to the conventional secondary fluid borehole that shows 17 to 26 m/kW with 20 mm to 50 mm pipe diameters. The seasonal COP of the heat pump increases by 21% for a 150% increase in borehole length. For the same scenario, the heating capacity of the heat pump increases by 15%. This demonstrates the importance of the borehole sizing on the efficiency of the heat pump.

This work shows the importance of the proper sizing of the heat pump capacity for a specific application. GSHPs show the lowest energy consumption, but ASHPs remain the most attractive heat pumping option for residential users. Future work on GSHPs should continue to address overcoming the high cost or achieving improved seasonal efficiency by meeting DHW loads in addition to space heating loads.

<u>Refrigerant Mixtures</u>

The use of refrigerant mixtures is becoming more and more common in air conditioning and refrigeration. In 1965, the ASHRAE Guide and Databook Fundamentals and equipment published three azeotropic refrigerant mixtures: R500, R501 and R502. In 2013, the 'ASHRAE Handbook Fundamentals' listed 65 zeotropic mixtures and 14 azeotropic mixtures. This number is growing each year. These new blends meet the need of the market which must deal with the phase-out and phase-down of CFCs, HCFCs and HFCs. To replicate the performance and characteristics of these refrigerants for specific applications it was necessary to create this diversity of mixtures.

One of the features of zeotropic blends is the temperature glide (Figure ES-14). At constant pressure, the mixture boiling temperature (bubble point) is lower than the condensing temperature (dew point). By matching the temperature glide of the refrigerant with the temperature glide of the fluid to cool in an air conditioning or chiller system, a 10 to 15% COP improvement can be achieved with a temperature glide of 5.5°C. If the application allows a temperature glide of 10°C, the COP of the heat pump could be improved by up to 30% theoretically.

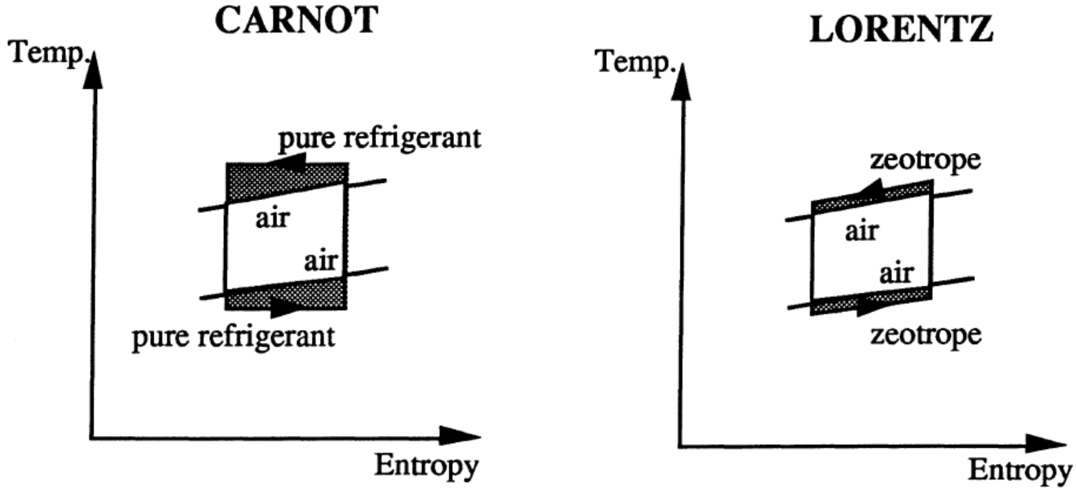

(a) (b)

Figure ES-14: (a) Typical Carnot refrigeration cycle (b) Lorentz cycle demonstrating temperature glide

A heat pump simulation model was developed to assess the benefits of different refrigerant blends without modifying the main heat pump system components: compressor, evaporator and condenser. Among all the mixtures studied, R32/CO_2 (80/20) mixture presents better performance potential for this study. The mixture is non-toxic with a GWP of approximately 540, which is 75% lower than the GWP of R410A. Moreover, it is a zeotropic mixture with approximate temperature glides of 6°C and 8.5°C in the evaporator and condenser respectively.

To assess the performance of various refrigerant mixtures, residential building energy models were used. Five refrigerant cases were simulated using the same heat pump components:

- Case 1 (reference case): Standard R410A air source heat pump, with a nominal heating capacity of 7.7 kW at 8°C outdoor temperature. This unit meets 75% of the total space heating load, so 25% of the load was provided by the auxiliary heating system.
- Case 2: Same as reference case with a variable speed compressor
- Case 3: Fixed mixture of 80% R32 and 20% CO_2
- Case 4: Variable composition (VC) mixture R32 - CO_2 with a reservoir located at the compressor suction to manage the concentration of CO_2
- Case 5: Fixed 80% R32 and 20% CO_2 with a variable speed compressor

The results of the simulation are summarized in Table ES-8 with the heat pump (HP) contribution indicating the percentage of the annual heating capacity met by the heat pump and the seasonal COP of the system.

Table ES-8: Simulation results for five refrigerant mixture cases

Refrigerant Case	Capacity	HP contribution	COP seasonal
	kW	kWh/kWh	kWh/kWh
R-410A	7.7	75%	2.16
R-410A VSD	7.7	91%	2.73
R32-CO2 80/20	8.1	84%	2.46
R32-CO2 VC	9.0	93%	2.81
R32-CO2 80/20 VSD	8.1	97%	2.98

These simulations show a potential COP improvement of ~14% (2.46 vs. 2.16) just by swapping the refrigerant in a heat pump. But, the COP could be improved by ~30% (2.81 vs. 2.16) if the basic mechanical design of the heat pump was modified to include VC control. In other words, to get the total benefit of the refrigerant mixture glide, the air flow rates and the air coils' circuiting should be revised or redesigned. The design of refrigerant mixtures is a promising approach for heat pumps COP improvement. The next steps in this project will be to confirm experimentally the performances predicted by the model and to design a heat pump unit adapted to refrigerant mixtures with a strategic temperature glide.

2.2.2 Laboratoire des Technologies de l'Energie (LTE) Contributions

Previous to its involvement in the Annex 41 program, Hydro-Québec's LTE had conducted laboratory and field testing of air-to-air and air-to-water heat pump systems (Dumont & Le Lostec, 2014). The lab testing involved a cold climate system design, and tests have been conducted for outdoor temperatures down to -25°C (-13°F). Field-tested systems included the cold climate design, conventional ASHPs, and ductless ASHPs.

LTE's R&D under Annex 41 focused on:

1. Quantifying efficiency improvements of traditional air-source heat pumps, ASHPs, utilizing cycle enhancements – two-stage and variable-speed compressors and vapor-injection
2. Analysis of the C656 standard (CSA (2006, 2014)), Canadian heat pump efficiency test standard, to understand its limits and identify areas for improvement

<u>Enhanced Air-Source Heat Pumps</u>

In order to foster the emergence of cold climate heat pumps on the market, efforts are being made at Hydro-Québec's energy technology laboratory (LTE) to characterize the equipment and propose solutions to promote the deployment of numerous air-source heat pump technologies.

The field test results of this study, shown in Figure ES-15, demonstrate that ASHPs installed according to current practices allow them to generate significant annual energy savings of between 25% and 30% in the case of conventional heat pumps and between 45% and 50% in the case of variable speed heat pumps as compared to resistive heating equipment. Variable speed heat pumps therefore generate greater energy savings than conventional heat pumps; however this remains difficult to precisely quantify due to the small number of samples. It is important to mention that the quality of the installation of heat pumps has an impact on the performance of the overall heating system. The airflow, refrigerant load and heating equipment controls (or the interaction between the various devices) are factors that should not be overlooked when they can have a significant impact on the generation of energy savings, and this applies for the entire life cycle of the equipment. Furthermore, unless a major problem occurs (a refrigerant leak for example), it is difficult for an individual to identify when a heat pump's operation is less than optimal because of poor installation practices.

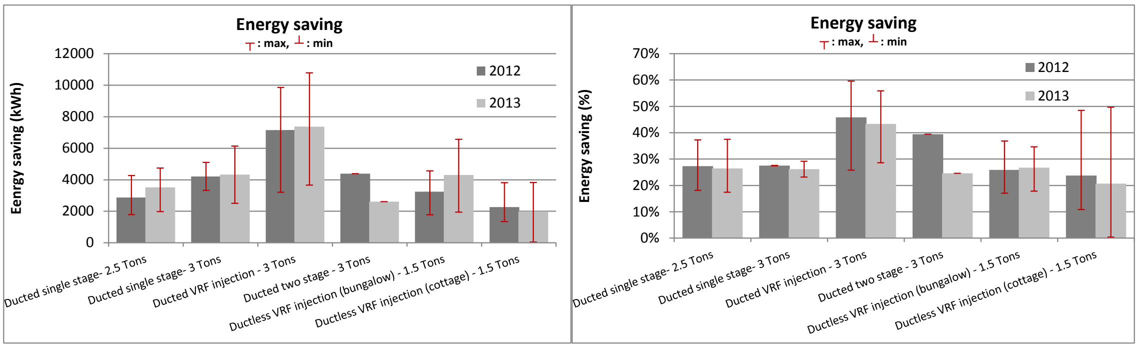

Figure ES-15: Energy savings by heat pump category

Our measurement campaign also demonstrated that rated HSPFs as defined by CAN/CSA-C656-05 (similar procedure as AHRI 210/240) is not a criterion adapted to represent energy savings although there is a link between the average coefficient of performance of the systems we studied and the HSPF. It should be noted that the Office of Energy Efficiency (OEE) issued a publication in 2010, *Bulletin on Reporting Cold Climate Performance* (http://www.nrcan.gc.ca/energy/regulations-codes-standards/bulletins/7177), recommending modifications to CAN/CSA-C656-05 so that the performance of heat pumps used in cold climates is better represented in the standard. One requirement from this modification was additional standard testing to report heating capacity and COP at -17.8°C (0°F) be put in place by January 1, 2014. This would require that standardization labs be in a position to meet the criteria of the tests proposed by the OEE.

CAN / CSA C656 Standard

If the HSPF is a selection criterion for a potential Program on heat pumps, it is important to know the limitations and work to close the gaps, either by modifying the calculation of HSPF and/or establishing criteria to meet the needs. HSPF, which is a standardized performance criterion, does not result in energy savings predictions that are representative of what is observed in the field. Moreover, with the advent of new technologies such as variable speed compressors with or without refrigerant injection (vapor or liquid), the current HSPF calculation procedure does not give a realistic energy saving difference between the different technologies (Figure ES-16). This is explained partly by the calculation assumptions which aim to idealize the operation of heat pumps below the balance point. For some heat pumps with variable speed, including wall units, low temperature standard capabilities (-8.3°C) are not always based on the maximum speed of the compressor. Therefore, it is difficult to rely on this criterion to identify the most efficient equipment.

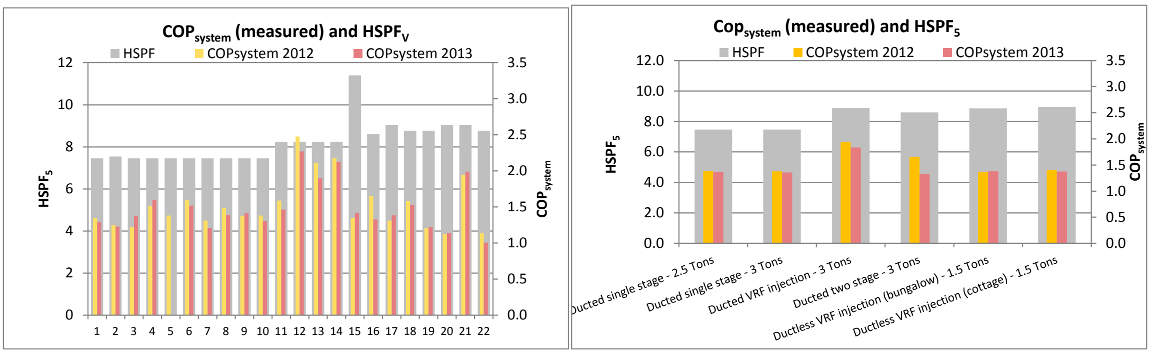

Figure ES-16: HSPF of heat pumps

In general, the modification of a standard is relatively tedious. Different actors have different interests that must be taken into account. For example, when revising the Energy Star label, manufacturers were concerned about the workload that could represent the addition of low temperature standardized tests and take into consideration regional weather conditions rather than national. Therefore, if an amendment to the C656 standard should be carried out, it would be appropriate that these changes are also made to the American AHRI 210/240 in order not to create obstacles to the development of the Canadian market. One way not to be overlooked is the job of Annex 39 of the IEA, which aims to standardize internationally the heat pump performance criteria.

2.3 Japan

Japan has a large Annex 41 team (Table ES-9) consisting of experts from national organizations for professional heat pump technology research.

Table ES-9: Japan Annex 41 team organization

Leader	
Prof. Katsuta, Waseda University	
Secretary	
Takeshi Hikawa (**HPTCJ)	
Board Members	
Prof. Koyama, Kyushu University	Prof. Ohkubo, Tamagawa University
Prof. Shikazono, the University of Tokyo	Prof. Saito, Waseda University
Prof. Fukuta, Shizuoka University	Associate Prof. Asano, Kobe University
Prof. Kagawa, National Defense Academy of Japan	Dr. Hashimoto, Central Research Institute of Electric Power Industy (CRIEPI)
Plus researchers from industries (Mitsubishi Electric, Mitsubishi Heavy Industries, Daikin, Toshiba Carrier, Hitachi Appliance), and electric power companies (Hokkaido Electric and Tokyo Electric)	
NEDO*: Official Contracting Party, Delegate to IEA Heat Pumping Technologies Program	

*NEDO: New Energy and Industrial Technology Development Organization
**HPTCJ: Heat Pump & Thermal Storage Technology Center of Japan

The annual energy consumption per household in the cold climate area of Japan (e.g., Hokkaido) is about 1.7 times as high as compared to that in the mild temperature area (e.g., Kanto or Tokyo). Space heating and water heating account for about 80% of the total energy usage (Figure ES-17) presenting a significant opportunity for energy and cost savings. Due to the energy conservation needs, several ASHP systems for cold climate areas were developed relatively early and already marketed in Japan. Japan's R&D contributions to Annex 41 have been primarily focused on better understanding of OHX frosting/defrosting performance to facilitate development of a heat pump system model with an improved OHX frost model. The new model is expected to help developed improved cold climate ASHP systems in the future. A number of early stage advanced system developments have also been described along with advances in properties research for R32 (a leading refrigerant candidate for future heat pumps, alone or in blends).

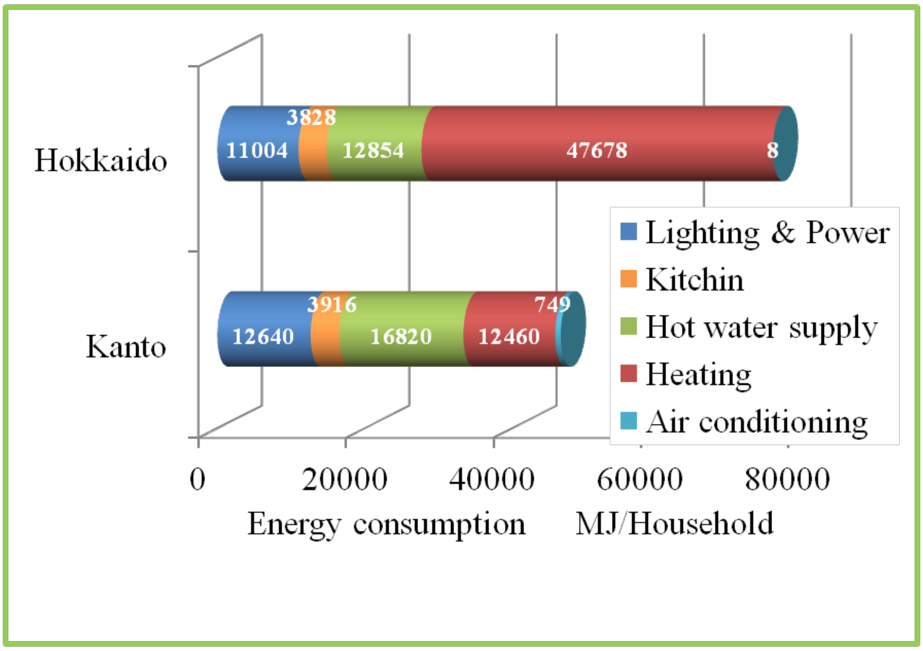

Figure ES-17: Annual energy consumption per household in the cold climate area

2.3.1 Task 1 literature & technology review

A comprehensive review was performed in primarily two areas: cold-climate heat pumps and fundamental research on frost formation in heat exchangers. Recent developments in R32 thermophysical property measurements and models were also reported.

The cold-climate heat pump review encompassed several publications that focused on the functionality and improvement of heat pumps and air conditioners working in cold climates (-25°C). Emphasis was given to novel architecture and packaging as well as heat exchanger modifications to improve performance. A number of ASHP products (mostly single-zone and multi-zone ductless types) with improved cold climate performance have been introduced to the market by Japanese manufacturers (Mitsubishi, Toshiba, Hitachi, Daikin, others). They employ a number of heat pump cycle innovations including variable speed compressor technology, vapor injected compressors, liquid injected compressors, etc. Rated performance characteristics show capability to maintain heating capacity at 70% to 90% of rated capacity down to -20°C to -25°C outdoor temperatures. Most meet the requirements of recently released cold climate heat pump specifications by the U.S. Northeast Energy Efficiency Partnership (NEEP). These developments demonstrate the technical feasibility to develop ASHPs with significantly improved cold climate heating performance compared to conventional products.

The second component of the literature review focused on fundamental frost formation simulations and calculations as well as experimental results for validation and discussion of various setup regimes that affect heat exchanger performance. The literature went on to detail models for frost formation and heat flux at different frosted conditions. Conclusions were drawn that wettability of the cooling surface significantly affected the physical force required for removal. In Tasks 2 and 3 the frost model was developed further and incorporated into an ASHP system model for use in analysis and design of future heat pump systems.

Finally, in order to use any refrigerant, especially a relatively new one like R32, reliable and accurate thermophysical property information is required. Accurate isobaric heat capacity (c_p) data is one of pieces of information needed to design application systems. Hozumi et al. (1994) reported speed of sound of gaseous R32 at temperatures from 273 K to 343 K and at pressures from 0.02 MPa to 0.25 MPa. Kubota et al. (1995) reported 18 R32 c_p measurements in the gas phase obtained from 303 K to 343 K and from 0.12 MPa to 0.5 MPa by using a flow calorimeter. Kagawa et al. (2012a) reported 32 c_p measurements similarly obtained from 274 K to 353 K and from 0.65 MPa to 2.4 MPa. More recently Kagawa et al. (2012b) reported on additional R32 c_p data obtained at temperatures from 282 K to 319 K and at pressures from 1.0 MPa to 2.4 MPa. These data sets have been used to evaluate several equations of state (EOS). In addition curves of the isobaric ideal-gas heat capacity ($c_{p,0}$) and the vapour saturation heat capacity (c_p") of R 32 were determined using the data (Kagawa et al, 2012b). The data along with the derived curves of $c_{p,0}$, and c_p" and the EOS evaluated are shown in Figure ES-18. These data will be very useful for improving available models so as to represent reliable thermodynamic properties of R-32 and refrigerant mixtures with R-32 that are used for cold climate A/C and heat pump systems.

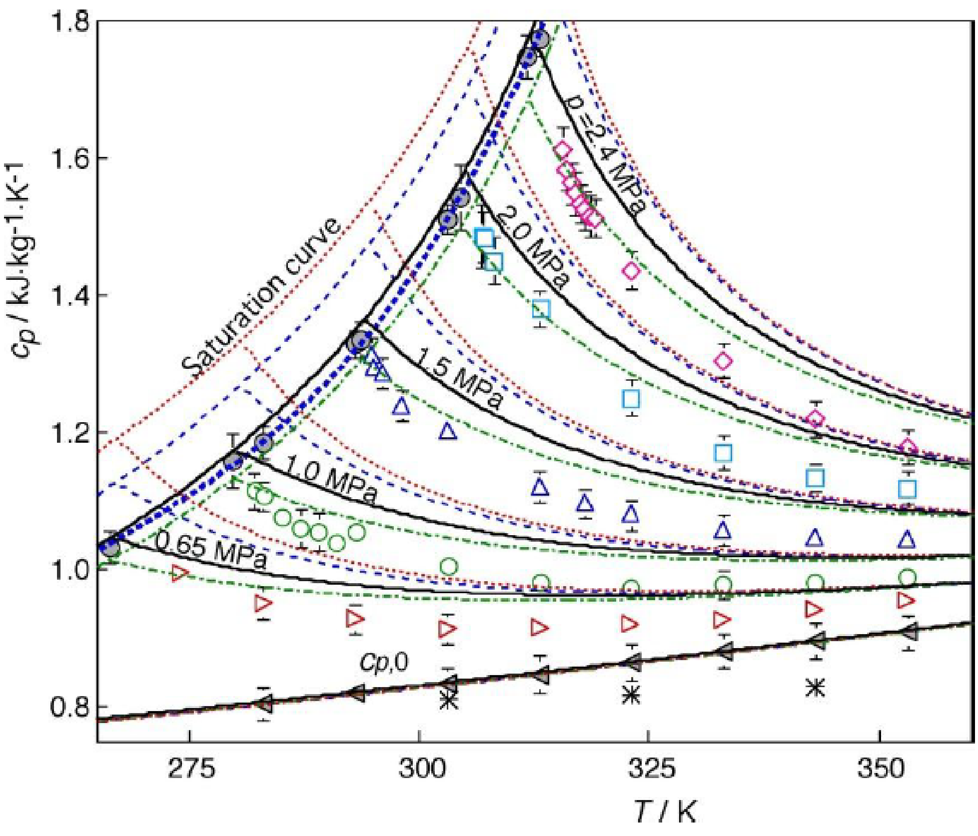

Data: open symbols from Kagawa et al. (2012a, b); * from Kubota et al. (1995)
Derived c_p" curve and data from Kagawa et al. (2012b)
EOS: Outcalt and McLinden (1995)
Tillner-Roth and Yokozeki (1997)
Piao and Noguchi (2001)
Astina and Sato (2004)

Figure ES-18: Isobaric heat capacity measurements for R-32 – experimental data (symbols) vs. several equations of state, EOS (lines)

2.3.2 Task 2 and 3 highlights

To further investigate potential improvements of refrigeration cycles in cold-climate operations, three principal areas of research were explored: frost formation simulation and validation, usage of thermosiphons to collect heat from ground layers, and frost free heat pump for water heating.

<u>Frost Formation Simulation and Experimentation</u>

A detailed analysis of frost formation in heat pump heat exchangers was performed in order to generate and validate a numerical model. Experimentation utilizing controlled inlet air temperature, inlet absolute humidity, cooling surface temperature, and initial flow rate was performed to analyze the frost formation and density across various geometries. In analyzing various parameters and their effect on frost formation, a numerical model was built to predict frost formation given different operating schemes.

In parallel to the modeling efforts, an experimental setup was created to validate the numerical model and also to perform optimization and apply improvements (Figure ES-19). The test equipment consists of a temperature-controlled air supply unit, blower, volume flow meter, test section, and ducts that connect these main units. In the temperature-controlled air supply unit, air temperature and humidity are adjusted to certain levels. The air is fed by the blower to the cooled test section, where frost forms between two flat plates. The air that has passed the test section returns to the temperature-controlled air supply unit for recirculation. The condition of air before and after the test section and the heat flux into the test section are measured. At the same time, frost layer heights are measured by means of image processing. A finless heat exchanger that has the shape as shown in Figure ES-20 was designed. This study used an aluminum test section that duplicates the air-side flow paths in an outdoor heat exchanger (OHX). Table ES-10 represents the test conditions while Table ES-11 and Figure ES-21 provide the design parameters and details of the test section, respectively.

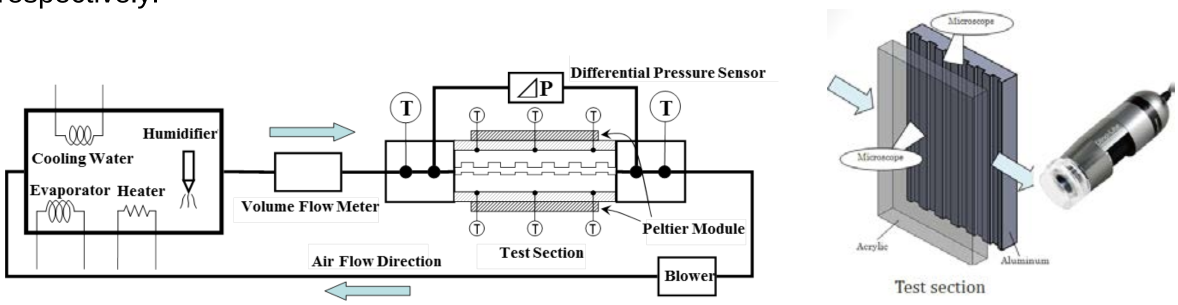

Figure ES-19: Schematic view of test equipment (left) and new visualization technique (right)

Table ES-10: Test conditions

Inlet air temperature T_a	ºC	7.0
Inlet absolute humidity X_a	kg/kg'	0.0053
Cooling surface temperature T_w	ºC	–10.0
Initial flow rate	m^3/h	5.0

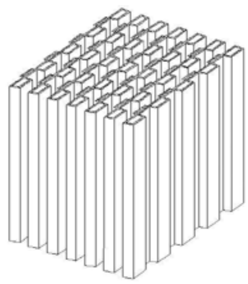

Figure ES-20: Overall view of heat exchanger

Table ES-11: Design parameters

		No.1	No.2	No.3
(1) Height of convex a_l	mm	2.0	1.2	2.8
(2) Depth of concave a_u	mm	2.8		
(3) Width of concave/convex l	mm	8.0		
(4) Pitch of convex/concave L	mm	16.0		
(5) Angle of convex/concave α	deg.	10		
(6) Number of convex/concave N		6		

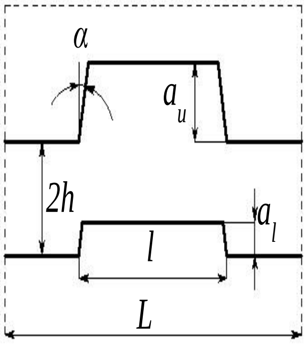

Figure ES-21: Concave- and convex-patterned test section details

From digital microscope images, the diameters and intervals of frost pillars are measured (see Figure ES-22 for example for test section No. 2), and the frost transition time is also specified. The visualization technique used provided a maximum resolution of 0.02 mm. The taller the convex height became, the higher the initial air velocity (the Reynolds number) became at the point where the flow path was narrow. As a result, initial frost pillar diameters and frost pillar intervals became smaller, indicating that the difference in initial air velocity (the Reynolds number) had an influence on the mode of frost pillar formation.

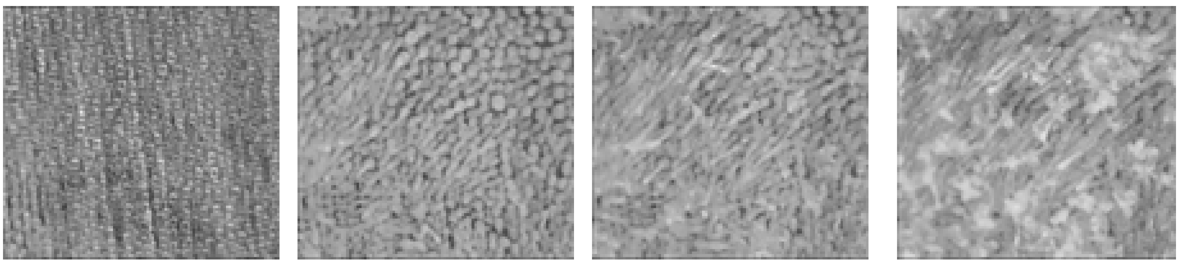

(a) 2min (b) 4min (c) 5min (d) 7min

Figure ES-22: Process of frost layer growth (No. 2)

Analysis of frost layer growth was conducted based on the calculation model suited for each frost layer growth process. Frost layer growth process is classified into three stages: "crystal growth stage," "frost layer growth stage," and "frost layer full growth stage." Because this test was not designed to analyze frost pillars melting on the frost layer surface, the analysis of the frost layer growth process was conducted based on the crystal growth stage and the frost layer growth stage.

Between the concave- and convex-patterned flat plates, the transition from water vapor to frost pillars occurs first in the upstream area and gradually moves toward the downstream area. Based on frost growth observation results, a transition period is practically defined as the time between the point when the mean frost layer height becomes about 0.10 mm and 80% of the time when the flow path becomes completely blocked. The point of the transition is calculated to shift linearly from the start to the end of the transition period. Figure ES-23 shows the comparison results of calculated and measured mean frost layer densities. Likewise, Figure ES-24 shows the comparison results of calculated and measured mean frost layer heights.

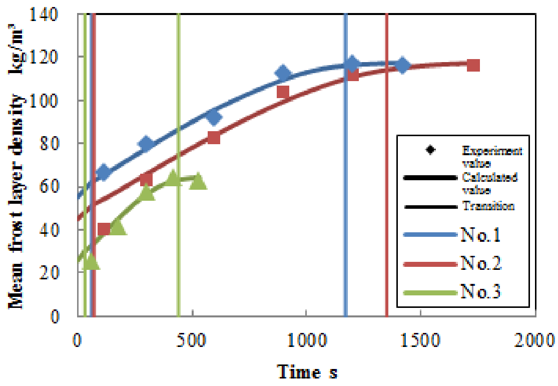

Figure ES-23: Comparison of mean frost layer density

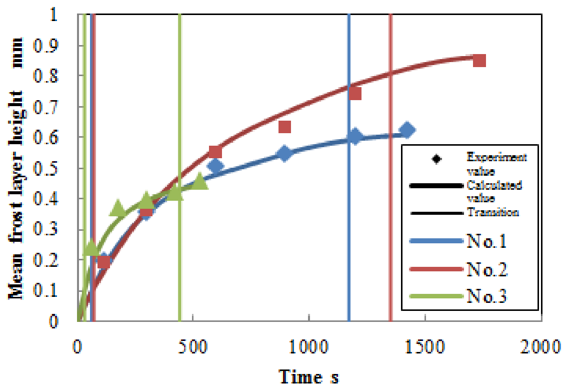

Figure ES-24: Comparison of mean frost layer height

In Task 3, the Japanese team extended the frost R&D work to apply the frost growth model in an ASHP system model and validate it with system test data. This study created a system model with the frost model embedded in heat exchanger routines. Figure ES-25 shows the results of frost weight changes, indicating that frost weight almost linearly increases with time. As shown in Figure ES-26, the numerical calculation of power consumption agreed with its experiment result relatively well.

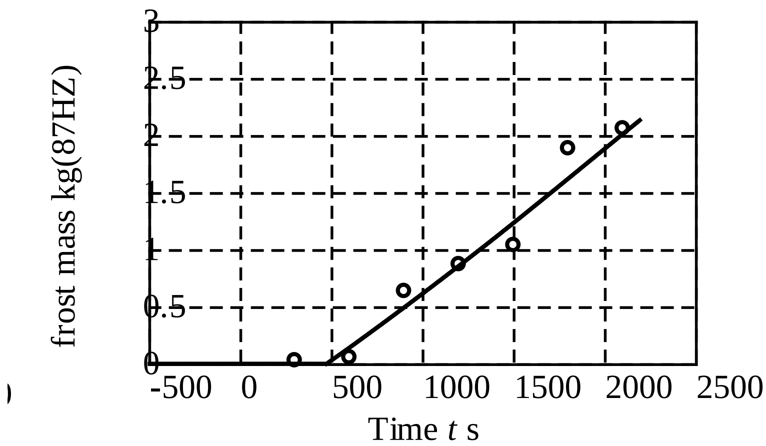

Figure ES-25: Frost mass

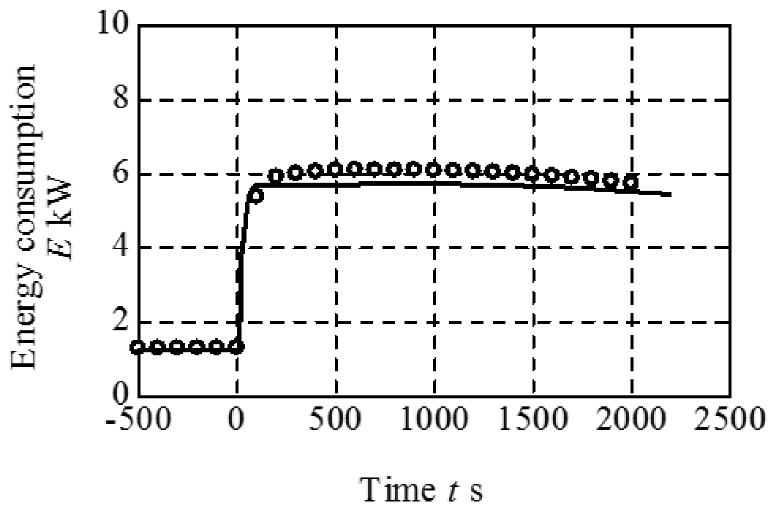

Figure ES-26: Energy consumption

<u>Use of Thermosiphons to Collect Heat from Ground Layers</u>

Thermosiphons with a new shape were designed and evaluated for their ability to collect ground heat for a GSHP system using CO_2 as the working fluid. Figure ES-27 illustrates the experimental apparatus and characteristics of the thermosiphon designs tested. An internal "showering" tube was used to promote wetting of the thermosiphon wall with liquid CO_2.

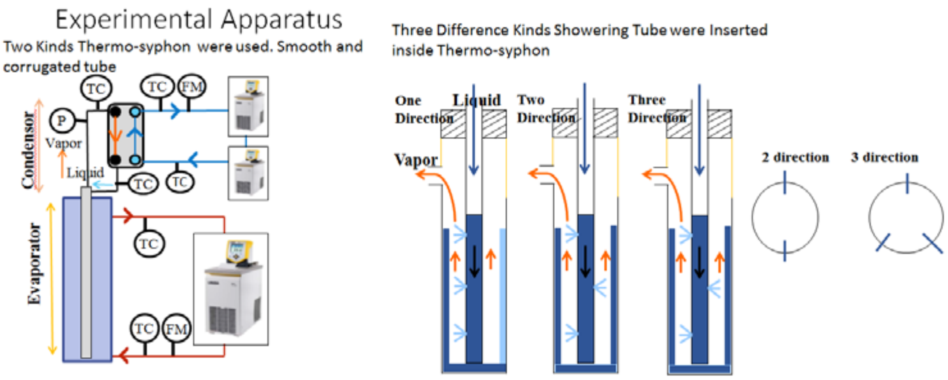

Figure ES-27: Thermosiphon tube test appratus schematic, left; and test evaporator characteristics, right

It was found that using smooth wall construction demonstrated better heat transfer than corrugated due to lower thermal barrier. Additionally, the length and number of thermosiphons was analyzed showing their improved effectiveness in different setups. Empirical relations were also used to explain the performance of the thermosiphon. The novel technology provided ample increase in COP in heat pump simulations. In the case where no showering tube is used, the number of thermosiphons required to achieve the targeted COP 2.8 is 14 for the tube length of 10 m, and 9 for 15 m (Figure ES-28). Similarly, in the case where a three-direction showering tube is used, the number of thermosiphons required is 13 for the tube length of 10m, and 9 for 15 m (Figure ES-29). Based on these results, in the case where 10-m-long thermosiphons are used, the use of a three-direction showering tube successfully reduced the number of thermosiphons required (in this connection, note that COP was calculated as annual performance factor (APF) here).

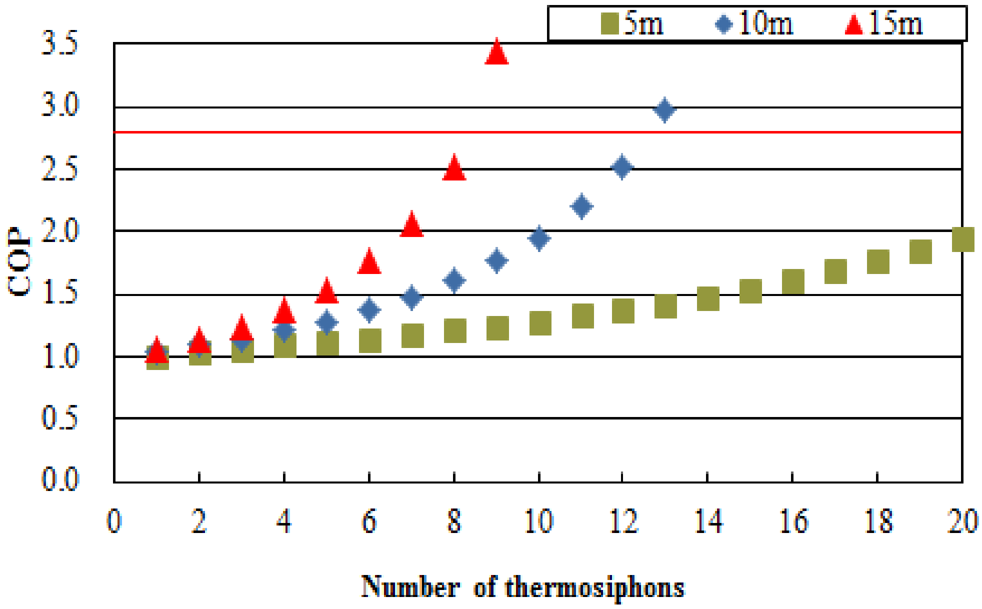

Figure ES-28: Results of heat pump simulations (smooth tubes without showering tube)

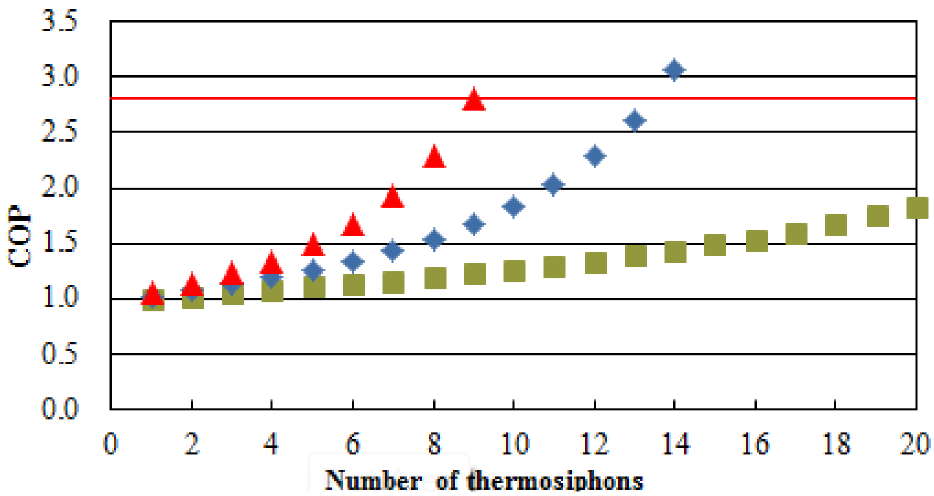

Figure ES-29: Results of heat pump simulations (smooth tubes with three-direction showering tube)

Frost Free Heat Pump for Water Heating

Air source heat pump water heaters (ASHPWHs) are widely applied as an economic form of heating. One of the largest problems in ASHPWHs is evaporator frosting, and the subsequent need for defrosting at a low ambient temperature and high relative humidity. We proposed a frost-free air- source heat pump water heater system with integrated solid desiccant, in which frost formation can be significantly mitigated by dehumidifying air before it enters the ASHPWH evaporator.

This system consists of a desiccant-coated refrigerant/air heat exchanger (1), an uncoated refrigerant/air heat exchanger (2), a compressor (3), a refrigerant/water heat exchanger (4), a water storage tank (5), a pump (6), two expansion valves (7, 8), a fan (9) and three air valves or dampers (10, 11, 12), as shown in Figure ES-30 (left side). With respect to the moisture moving in the desiccant, the operation process of the ASHPWH system can be classified into two modes: adsorption mode (AD mode) and desorption mode (DE mode). In AD mode, both (1) and (2) are evaporators with the air valve 10 closed and valves 11 and 12 open. Outdoor air is drawn across both evaporators and dehumidified by the desiccant coating on (1).

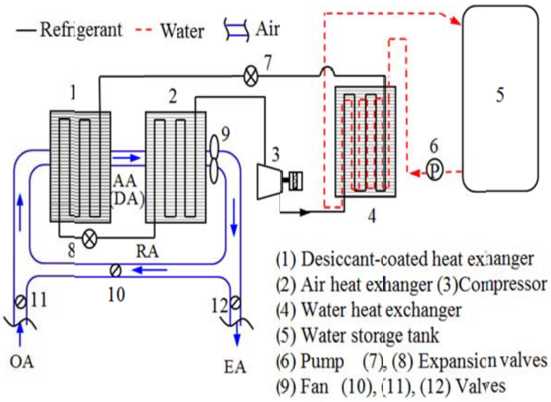

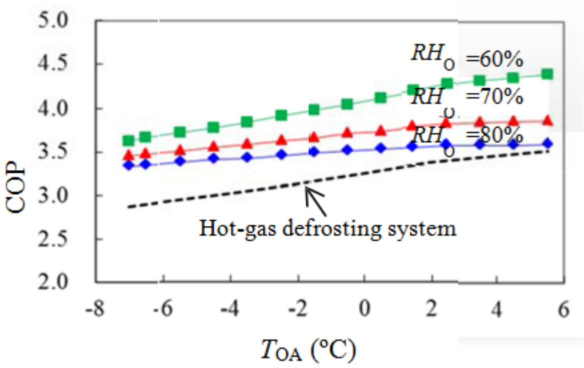

Figure ES-30: Schematic diagram of the frost-free AS HPWH system (left) and performance simulation results (right)

During DE mode, the expansion valve (7) is opened and another expansion valve (8) throttled. Therefore (1) becomes a condenser, and (2) remains an evaporator. Simultaneously, air valve (10) is opened and valves (11, 12) closed to form a closed air cycle between (1) and (2). The refrigerant exiting from compressor (3) initially transfers part of its heat into the water at (4), and then dissipates the remainder at (1), regenerating the desiccant coating and heating and moisturizing the return air (RA) to state DA. The hot and humid air (DA) is then passed through (2), in which the refrigerant is vaporized by obtaining heat from DA, and finally, leaves at state RA. Therefore, the total heat load added to DA in (1), including sensible and latent heat, could be completely recycled in (2). As a result, zero heat loss at the air side and continuous heat output to water are realized. Because the released moisture is exhausted at (2), the evaporation temperature of the refrigerant in (2) must exceed 0°C while in DE mode. A single period is ended when this moisture adsorbed by the desiccant in AD mode is completely discharged in DE mode.

The effectiveness of this system has been analyzed experimentally and numerically. Figure ES-30 (right side) illustrates the results that about a 20%-30% boost in COP could be achieved at a temperature of -7°C and relative humidity of 60-80%. This technology is also applicable to other air source heat pumps for heating, etc.

2.4 United States

U.S. CCHP R&D efforts described in the Task 1 and Task 2/3 reports focused on analyses and experimental (lab and field) investigation of several advanced VC cycles for ASHPs. Vapor injection (VI) cycle concepts, two-capacity compressors, variable speed (VS) compressors, parallel compressors, two-stage cycles with economizers, an oil-flooded compressor cycle concept, and several other advanced cycle approaches have been investigated. Based on early stage analyses, three CCHP cycle concepts were identified as among the most promising for meeting the goals – two-stage economizer cycle, oil-flooded compressor cycle, and a single-stage cycle using parallel compressors.

A brief summary of current promotional efforts for advanced ASHP systems, including CCHP applications, is given at the end of this section.

2.4.1 Two-stage economizer system

A field test of an advanced two-stage ASHP designed for cold climate operation has been completed at Camp Atterbury, a U.S. Army base outside Edinburgh in Indiana (Caskey et al., 2013). The heat pump is a two-compressor (two-stage) system with an economizer VI loop, similar to the concept analyzed by Bertsch et al. (2008). It featured a large tandem scroll compressor (two parallel compressors) for capacity boosting during low ambient temperature heating operation and a variable speed scroll compressor for cooling operation and moderate ambient temperature heating. The test was conducted under the DOD's Energy Security Technology Certification Program (ESTCP). Two identical military barracks from available buildings located at Camp Atterbury were selected for the field demonstration. The originally installed HVAC system was a natural gas furnace with a split system A/C. A side-by-side performance comparison between the originally installed HVAC systems and the two pre-commercial heat pump units developed at Purdue University was conducted during the 2012-2013 heating season. The heat pump units had a design heating capacity of 18.34 kW (62,580 BTU/h) at an ambient temperature of -20^{o}C (4^{o}F).

The heat pump performance was compared to the existing HVAC system. For the monitored period at the Army site the ASHP system achieved approximately 19% source energy savings vs. the baseline gas furnace system but utility costs were higher due to the low price the Army pays for natural gas at the site. Using average Indiana residential electricity and gas prices, the utility costs for the ASHP and baseline furnace would have been comparable. This operation cost equivalence despite the energy savings of the ASHP is because the price for natural gas in Indiana is about one-third that of electricity per unit of energy delivered, which is true of most locations in the United States. The ASHP used no electric backup heating during the test period. Using ASHRAE Standard 55 (ASHRAE, 2010) to evaluate the thermal comfort indicated that the heat pump was able to maintain comfort levels throughout the heating season. Furthermore, while the first cost of the two-stage ASHP will be higher than that of a conventional single-stage ASHP, the installation and maintenance costs are estimated to be comparable.

2.4.2 Two-port vapor injected compression with regeneration

Additional research at Purdue University's Herrick Labs focused on the experimental investigation of a commercially available 17.5 kW (5-ton) heat pump that was retrofitted with a two-port vapor injected scroll compressor. The injection ports within the two compression pathways were located in the fixed scroll with different distances from the suction chamber. The vapor at the two injection pressure levels was generated using two flash tank separators in a cascade configuration. This configuration made it necessary to not only control the superheat but also the liquid levels in the separators and subcooling of the refrigerant leaving the condenser.

Baseline performance data of the heat pump without vapor injection was obtained and compared with test data obtained for the two-port vapor injection system. For the baseline, the injection lines to the compression pockets were plugged within the fixed scroll to reduce dead volume and re-expansion losses. Also, the vapor-separator section was shut off and bypassed. In the second step, the plugs were removed and a staged expansion process was performed using the separator section. The generated vapor from each separator was injected into the respective compressor port causing an intercooling effect on the compression process.

With identical compressor speed, a 28% improvement in capacity was achieved at the 8.33°C design point, when compared to the baseline without vapor injection. When the baseline and vapor injected system capacity were matched by adjusting compressor speed, the COP increased by up to 6% at -8.33°C. Results of a bin-type analysis of the experimental results predict an improvement in the heating seasonal performance factor (HSPF) of 6% for Minneapolis and nearly 7% for ANSI/AHRI 210/240 cold climate region V.

2.4.3 Oil-flooded compressor system

Further research at Purdue University's Herrick Labs focused on the experimental investigation conducted with a commercially available 17.5 kW (5-ton) heat pump that was retrofitted with oil-flooded compression and regeneration. The indoor coil face area was kept unchanged while an additional heat exchanger was added as the oil cooler in the air flow path. In addition, a counter-flow plate heat exchanger with low pressure drops was used as the regenerator. Figure ES-31 provides a schematic and p-h cycle diagram for the schematic.

The results show that high oil circulation rates remove heat of compression and significantly reduce discharge temperature. By injecting oil in the compression process and using internal regeneration, the improvements in COP and heating capacity range from 4% to 15% and from 1% to 19%, respectively, depending on the oil mass fraction and operating temperatures compared with a conventional heat pump (without regenerator and without oil injection). As shown in Figure ES-32, oil circulation had little impact on heating capacity at the nominal rating operation condition (8.3°C), and the highest capacity improvement was observed at lowest ambient temperature (-17.8°C).

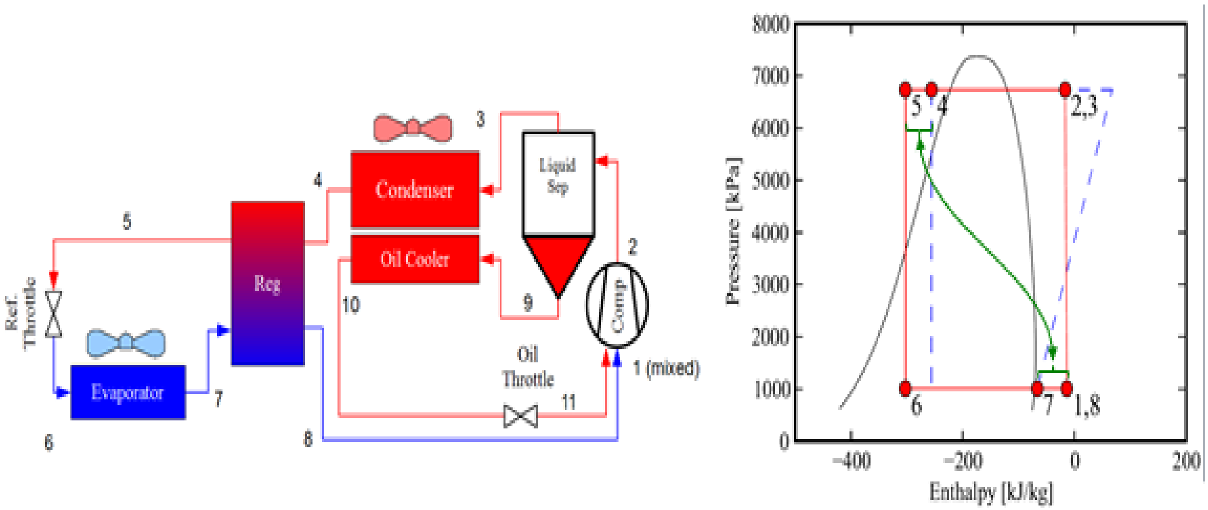

Figure ES-31: Schematic (left) and p-h cycle diagram (right) of flooded compressor cycle concept -from Bell et al. (2011)

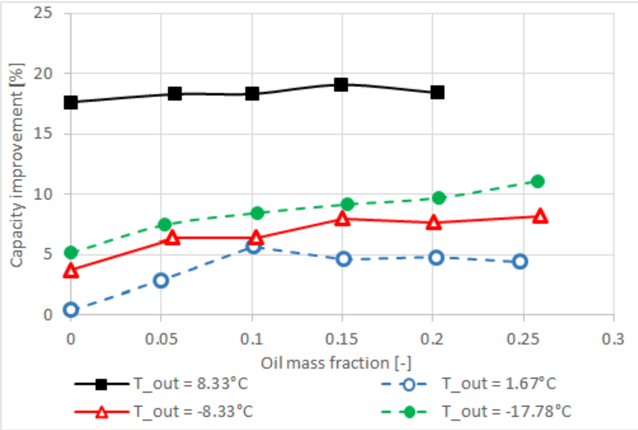

Figure ES-32: Capacity improvement between oil-flooded system with regeneration and baseline system

2.4.4 Single-stage ASHP with two parallel compressors

Analyses and lab evaluations led to development of a prototype ASHP featuring a pair of equal size, single-speed scroll compressors (one for cooling and mild ambient heating; both for cold ambient heating), see schematic in Figure ES-33. A laboratory prototype test system was built by modifying a 17.5 kW (~60,000 Btu/h or 5-ton) rated cooling capacity, single-speed, conventional ASHP and replacing its original compressor with a pair of equal size, single-speed compressors providing 10.6 kW (~36,000 Btu/h or 3 tons) of rated cooling capacity by operating only one compressor in cooling mode. Lab-measured performance indices indicated that the designs under investigation maintained their seasonal performance well over the full range of house performance levels. By comparison, the single-speed baseline loses 23% in seasonal performance in Region IV between the DHRmin (rated) and DHRmax heating load lines.

Based on the promising lab results, a prototype CCHP using parallel heating-optimized scroll compressors was constructed and installed in an occupied, single-story ranch home in central Ohio in January 2015 for field testing. The prototype (outdoor section pictured in Figure ES-34) replaced the original home HVAC system – a conventional single-speed ASHP with rated cooling capacity of ~10.0 kW (34000 Btu/h) at 35°C (95°F) and heating capacity of ~10.3 kW (35000 Btu/h) at 8.3°C (47°F), equipped with a 19.5 kW supplemental resistance heater for second stage and full back-up heating.

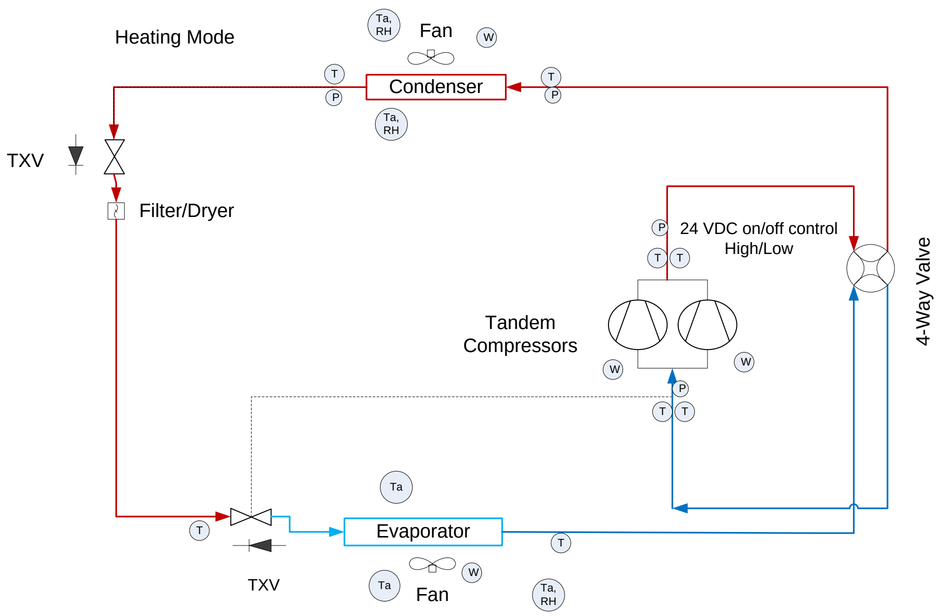

Figure ES-33: Field test prototype CCHP refrigerant schematic

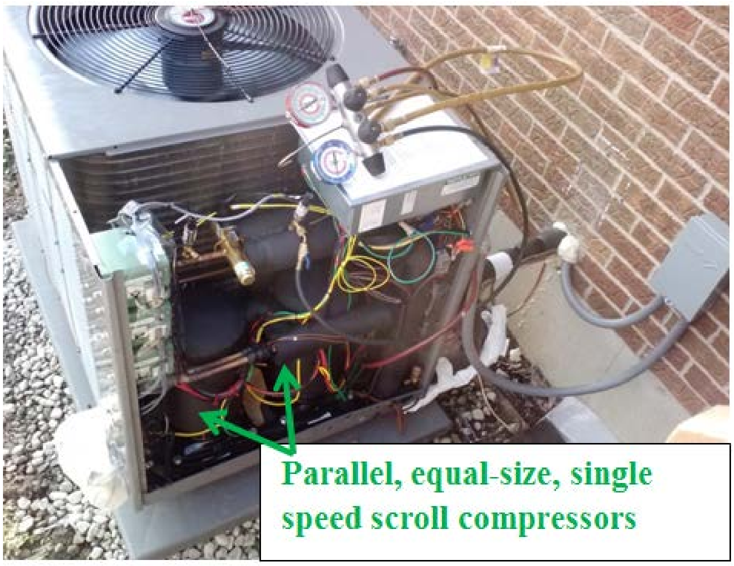

Figure ES-34: Prototype (using two compressors) being installed for field testing in a US residence

Field tests of the prototype in 2015 and 2016 demonstrated an average measured seasonal heating COP of about 3.0 and realized energy savings of more than 40% in comparison to a conventional ASHP during the coldest month (average temperature ~-7°C; minimum temperature -25°C). Results showed that at -25°C the unit had enough heating capacity that no backup heat was required (see Figure ES-35) at the test house. It is encouraging to see that, at -25°C, the field-measured COP was 2.2, i.e. 120% more efficient than resistance heating.

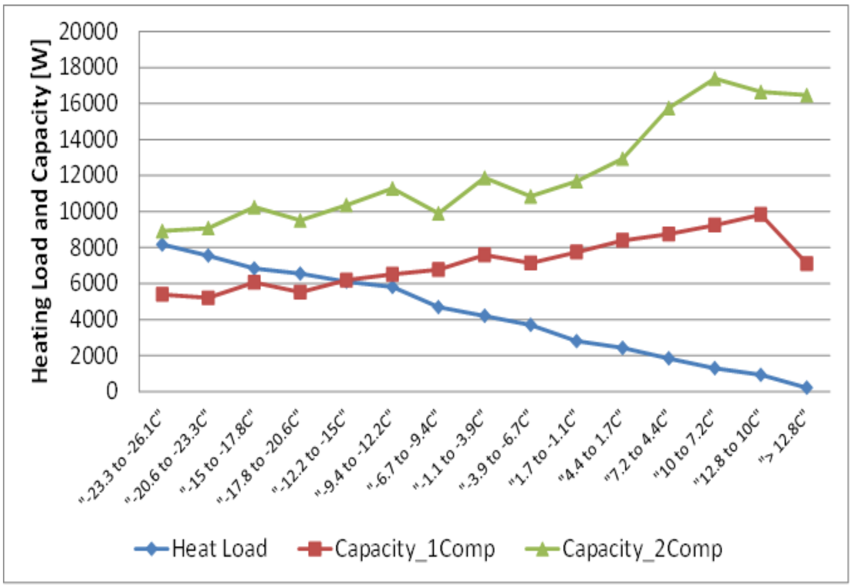

Figure ES-35: Two compressor CCHP prototype: measured average heating capacity (for 1 and 2 compressors) and building heat load vs. outdoor temperature

2.4.5 Complementary CCHP Market Promotion Activities

The US Northeast Energy Efficiency Partnership (NEEP) established a voluntary specification for cold climate ASHPs to help promote wider use of heat pumps in the northern parts of the US and the Northeast area. The specification was initially established in late 2014 with the most recent update effective January 1, 2017, and can be downloaded from the NEEP web site http://www.neep.org/initiatives/high-efficiency-products/emerging-technologies/ashp/cold-climate-air-source-heat-pump. It covers only air-to-air type variable-speed ASHPs (AWHPs and GSHPs are excluded). In order to be listed as complying with the NEEP specification, manufacturers' products must have a rated SCOPh ≥2.93 (US HSPF ≥10) for US climate region IV (moderate heating requirements) per AHRI Standard 210/240. In addition they must report space heating capacity and COP (from laboratory test data or engineering data) for at least 8.3°C, -8.3°C, and -15°C (47°F, 17°F, and 5°F) and at lower temperatures if available.

As of March 24, 2017, nearly 300 individual variable-speed ducted and ductless heat pump models were listed as complying with the latest NEEP CCHP specification V2.0. The list can be downloaded from the link above. Over 80% of the products listed are ductless types, either single-zone (2.6 to 9.4 kW nominal heating capacity) or multi-zone (2.9 to 14.1 kW nominal capacity). The remainder are centrally ducted (US type central air distribution systems) of about 6.5 to 16.5 kW nominal heating capacity.

The Electric Power Research Institute (EPRI) has also developed a specification for advanced ASHPs or Next Generation Heat Pumps (NextGen) (Domitrovic, 2017). This specification has two different levels or tiers. Under Tier 1 ASHP products must meet the same SCOPh requirement as for the NEEP specification above (≥2.93) but must also have space heating capacity at -8.3°C ≥80% of the rated capacity at 8.3°C. Under Tier 2, products must have a rated SCOPh ≥3.81 (US HSPF ≥13) for US climate region IV and a space heating capacity at -15°C ≥80% of the rated capacity at 8.3°C. Only about 7% of the products listed on the NEEP website currently meet the more stringent Tier 2 requirements.

3 ANNEX 41 FUTURE RESEARCH NEEDS

Numerous suggestions for future exploration have been identified by the participants as a result of Annex 41 efforts. Several of these are listed in brief below.

- Austria
  - Further experimental testing of other promising heat pump cycles
  - Detailed evaluation of an ejector cycle due to the promising results of the simplified modelling.
  - Improved compressor model for the LI cycle in order to improve the accuracy of the simulation results.
  - The measurement of the frost performance of the heat exchanger within the entire evaporator heat pump unit, including the quantification of the spatial frosting distribution. This will be linked to the change of acoustic emissions due to subsequently icing of the heat exchanger. This topic will be covered in the newly established Annex 51 (Acoustic Signatures of Heat Pumps), which started in April 2017.
- Canada
  - Semi-Virtual Test Bench for Measuring Heat Pump Performance
    - Will allow better understanding of interaction between heat pumps, the buildings where they are located, and the conventional resistive heating devices that are also present in the buildings
    - Also enables analysis of the control algorithms implemented in the thermostats.
  - Heat Pump Sizing Effort
    - Assess the sizing of heat pumps in Quebec (C656, F280, C273.5, rule of thumb, land characterization, market analysis ...) so that the sizing proposed by the C656 Standard is representative of Quebec situations and Canada.
  - Hybrid Ejector – Compressor Heat Pump
    - Based on the appropriate integration of compressor and ejector technologies using air as a heat source
    - Effort is now directed towards the development of a better ejector for R-134a (current ejector in test bench was designed for R410a) that will lead to higher entrainment ratios.
  - Solar-assisted Heat Pump
    - Investigate alternative ice generation approaches to lower equipment costs and increase maximum possible ice fractions
    - Evaluate system for larger buildings (multi-unit residential, office buildings) to examine different ratios of collector and storage area to building thermal loads
    - Evaluate potential of combining ice storage with liquid-based Building Integrated Photovoltaic/Thermal (BIPVT) system.
  - CO_2 Ground Source Heat Pump
    - Address overcoming the high cost of achieving improved seasonal efficiency by meeting DHW loads in addition to space heating loads
  - Refrigerant Mixtures
    - Confirm experimentally the performance predicted by the simulations with a prototype heat pump lab unit adapted to refrigerant mixtures with a strategic temperature glide.
- Japan
  - Build on frost modeling and testing work by conducting numerical simulations on repeated frost/defrost cycles to facilitate development of more efficient

heat pump operational methods and future ASHP systems with improved heating performance.
    - Propose feasibility research on the commercial practical use of thermosiphon evaporator GSHP in Hokkaido to embed heat pipes and try heat recovery using foundation piles. Both new construction and rennovation applications will be a target for this research
    - Design and build a prototype of the frost-free heat pump system, and test its performance
- United States
    - Parallel Compressor Prototype CCHP
        - Evaluate concept for other heat pump types (e.g. air-water ASHP, Brine/water-to-water, etc.)
    - Vapor-injected Compression with Economizing System
        - In the tested configuration, the injection ports did not include check valves. This is most likely the cause for the smaller performance improvement than predicted by the simulations.
    - Evaporator R&D
        - A larger fin pitch and tube diameter should be used for cold climate heat pumps to reduce the effects of frostbuild-up and refrigerant side pressure drop.
    - Oil-flooded Heat Pump Concept
        - Determine optimal circulating oil mass fraction as a function of outdoor temperature and superheat
        - Control superheat at inlet of compressor to allow the refrigerant to leave the evaporator as two-phase flow and to be superheated in the regenerator

4 REFERENCES

Astina, I.M., Sato, H., 2004, “A Rational Helmholtz Fundamental Equation of State for Difluoromethane with an Intermolecular Potential Background,” Int. J. Thermophys., Vol. 24, pp. 963-990.

Bell I. H., E. A. Groll, and J. E. Braun. 2011. “Performance of Vapor Compression Systems with Compressor Oil Flooding and Regeneration,” *International Journal of Refrigeration*, Vol. 34, No. 1, pp. 225-233.

Domitrovic, R., Personal communication to Van Baxter, April 2017.

Hakkaki-Fard, A., Z. Aidoun, P. Eslami-Nejad, (2016). Evaluation of refrigerant mixtures in three different cold climates residential air-source heat pumps, ASHRAE Transactions, Vol 122, Part 2, June 2016.

Hakkaki-Fard, A., Z. Aidoun, and M. Ouzzane, Applying refrigerant mixtures with thermal glide in cold climate air-source heat pumps, Appl. Therm. Eng., 62, 2014, pp. 714-722.

Hengel, F., R. Rieberer, A. Heinz, 2013. Theoretische Analyse zur Effizienzsteigerung durch Drehzahlregelung und Economizer-Schaltung bei einer Luft/Wasser Waermepumpe, DKV-Tagung, Hannover, AA IV.10.

Hozumi, T., Sato, H., Watanabe, K., 1994, “Speed of Sound in Gaseous Difluoromethane, J. Chem. Eng. Data,” 39, pp. 493-495.

Kagawa, N., Matsuguchi, A., Watanabe, K., 2012a, "Measurements of Isobaric Heat Capacity of R32", Int. J. Refrig., Vol. 35, pp. 1014–1020.

Kagawa N, Matsuguchi A, Yamaya K, Watanabe K. Behavior of isobaric heat capacity of r 32 in the gas phase, 2012b, Proc. the 6th Asian Conference on Refrigeration and Air Conditioning Paper No.2954 (Xi' an, 8/27/2012).

Kubota, H., Sotani T., Kunimoto Y., 1995, "Isobaric Specific Heat Capacity of Difluoromethane at Pressure up to 0.5MPa", Fluid Phase Equilibria, Vol. 104, 413-419.

Le Gall, R., J.M. Grillot and C. Jallut, "Modelling of Frost Growth and Densification", Int. J. of Heat Mass Transfer. 28,(7) (1997), 3177-3187.

Moisi H., Rieberer R.; Fleckl T., Popovac M., Reichl Ch., 2015: IEA HPP-Annex41, Task 2-Simulation Models and Prototype Experiments, Task-2 Report, Graz, Vienna.

Northeast Energy Efficiency Partnerships, 2017. "Cold Climate Air Source Heat Pump." Accessed June 2017. http://www.neep.org/initiatives/high-efficiency-products/emerging-technologies/ashp/cold-climate-air-source-heat-pump.

Natural Resources Canada (NRCan), 2010. "Bulletin on Reporting Cold Climate Performance." Office of Energy Efficiency Bulletin 7177.

Outcalt, S.L., McLinden, M.O., 1995, "Equations of State for the Thermodynamic Properties of R32 (Difluoromethane) and R125 (Pentafluoroethane)," Int. J. Thermophys., Vol. 16, 79-89.

Piao, C.-C., Noguchi, M., 2001. "Thermodynamic Properties of HFC-32 (Difluoromethane)," Int. J. Refrig., Vol. 24, pp. 519-530.

Popovac, M., S. Seichter, C. Reichl, P. Benovsky, 2015a. Implementation and application of the frost growth and densification model for numerical analysis of heat pump frosting performance Ammonia and CO_2 Refrigeration Technologies, April 16-18, 2015, Ohrid, Republic of Macedonia.

Popovac, M., S. Seichter, P. Benovsky, T. Fleckl. Ch. Reichl, 2015b. Numerical Analysis of the Frosting Performance of the air-side of a heat-pump, 24th IIR international congress of refrigeration, August 16-22, 2015, ICR2015, Yokohama, Japan.

Ramaraj, S., Braun, J.E., Groll, E.A, and Horton, W.T. (2016). "Performance analysis of liquid flooded compression with regeneration for cold climate heat pumps," Int'l J. Refrigeration, Vol. 68, August 2016, Pages 50–58.

Reichl, Ch., A. Strehlow, T. Oltersdorf, S. Braungardt, M. Pröhl, P. Benovsky, M. Popovac, T. Fleckl, GreenHP: Next Generation Heat Pump for Retrofitting Buildings – new evaporator component for large capacity air-to-water heat pumps, Advanced HVAC & Natural Gas Technology Conference, May 6-9, 2015, Radisson BLU Hotel Latvija Conference Center, Riga, Latvia; DOI: 10.7250/rehvaconf.2015.015; page 100-109.

Shen B. et al. Field Investigation of an Air-Source Cold Climate Heat Pump. Paper no. P.1.5.6 in the Proceedings of the 12th IEA Heat Pump Conference 2017, May 15-18 2017, Rotterdam, Netherlands.

Shen, B., O. A. Abdelaziz, and C. K. Rice. 2014. "Compressor Selection and Equipment Sizing for Cold Climate Heat Pumps," paper no. P.6.11 in the Proceedings of the 11th IEA Heat Pump Conference 2014, May 12-16 2014, Montréal (Québec) Canada.

Strehlow A., C. Martín-Callizo, T. Oltersdorf, M. Popovac, Ch. Reichl. GreenHP: Heat Exchangers for Next Generation Heat Pump, 4th International Congress and Exhibition on Aluminium Heat Exchanger Technologies for HVAC&R, 10-11 June, 2015, Hotel Radisson Blu Scandinavia, Düsseldorf, Germany.

Tamasauskas, J., Poirier, M., Zmeureanu, R., and Sunye, R., Modeling and Optimization of a Solar Assisted Heat Pump Using Ice Slurry as a Latent Storage Material Solar Energy, Solar Energy, 86(11), pp. 3316-3325, (2012).

Tao, Y. X., Mao, Y., and Besant, R. W., 1994, "Frost Growth Characteristics on Heat Exchanger Surfaces: Measurement and Simulation Studies," Proceedings of the 1994 ASME International Mechanical Engineering Congress and Exposition, Chicago, IL, Nov. 1994, HTD-Vol 286 , pp. 29–38.

Tillner-Roth, R., Yokozoki, M., 1997, "An International Standard Equation of State for Difluoromethane (R-32) for Temperatures from the Triple Point at 136.34 K to 435 K and Pressures up to 70 MPa," J. Phys. Chem. Ref. Data, Vol. 25, pp. 1273-1328.

Yamashita, K. "Frost phenomena under the Low Temperature Environment" Ph.D. Thesis, Tamagawa University, (2009) (in Japanese).

Yang, B., Blatchley, T., Bach, C.K., Braun, J.E., Horton, W.T., and Groll, E.A., "Application of Oil Flooded Compression with Regeneration to a Packaged Heat Pump System," Proc. of the 15th Int'l Refrig. and Air Cond. Conf. at Purdue, Paper 2631, Purdue University, West Lafayette, IN, July 14-17, 2014, 10 pages.

Yasui K., et al. Study on the Frosting Phenomena between Concavity and Convexity Plate under Forced Convection – Detailed Observation and Analysis of Frost Layer Growth. Paper no. O.1.6.2 in the Proceedings of the 12th IEA Heat Pump Conference 2017, May 15-18 2017, Rotterdam, Netherlands.

Zhang L. et al. A new method for preventing air-source heat pumps and refrigerators from frosting. Paper no. O.1.6.3 in the Proceedings of the 12th IEA Heat Pump Conference 2017, May 15-18 2017, Rotterdam, Netherlands.

Zoier, H., 2014: Betriebsverhalten von Aussenluft-Waermepumpen bei tiefen Aussenlufttemperaturen, Masterthesis, Institute for Thermal Engineering, TU-Graz.

Zottl, A., GreenHP Project Final Report, 01/12/2012 to 30/08/2016. AIT Austrian Institute of Technology. http://cordis.europa.eu/docs/results/308/308816/final1-fp7-308816-greenhp-publishable-final-report.pdf.

IEA Heat Pump Centre
c/o RISE - Research Institutes of Sweden
PO Box 857
SE-501 15 BORÅS
Sweden
Tel: +46 10 516 5512
E-mail: hpc@heatpumpcentre.org

HPT-AN41-SUM

www.heatpumpingtechnologies.org